SQT

NASA CR-134846

QUIET CLEAN SHORT-HAUL EXPERIMENTAL ENGINE (QCSEE) UNDER-THE-WING ENGINE COMPOSITE FAN BLADE PRELIMINARY DESIGN TEST REPORT

September 1975

by

Advanced Engineering & Technology Programs Department
General Electric Company

Prepared For

National Aeronautics and Space Administration

NASA Lewis Research Center
Contract NAS3-18021

1. Report No.	2. Government Accession No.	3. Recipient's Catalog No.
CR 134846		Engine (QCSEE)

4. Title and Subtitle	5. Report Date
QUIET CLEAN SHORT HAUL EXPERIMENTAL UTW COMPOSITE FAN BLADE PRELIMINARY DESIGN TEST REPORT	May 1975
	6. Performing Organization Code
7. Author(s) Advanced Engineering and Technology Programs Dept. Group Engineering Division	8. Performing Organization Report No. R75AEG411
	10. Work Unit No.
9. Performing Organization Name and Address General Electric Company 1 Jimson Road Cincinnati, Ohio 45215	11. Contract or Grant No. NAS 3-18021
	13. Type of Report and Period Covered Contractor Report
12. Sponsoring Agency Name and Address National Aeronautics and Space Administration Washington, D.C. 20546	14. Sponsoring Agency Code

15. Supplementary Notes

Test Report, Project Manager, C.C. Ciepluch, QCSEE Project Office
Technical Adviser, Morgan Hanson
NASA Lewis Research Center Cleveland, Ohio 44135

16. Abstract

This report presents the results of tests conducted on preliminary design polymeric-composite fan blade for the Under The Wing (UTW) QCSEE engine.

During this phase of the program a total of 17 preliminary QCSEE UTW composite fan blades were manufactured for various component tests including frequency characteristics, strain distribution, bench fatigue, dovetail pull, whirligig high cycle fatigue, whirligig low cycle fatigue, whirligig strain distribution, whirligig overspeed and whirligig impact. All tests were successfully completed with the exception of whirligig impact tests. Improvements in local impact capability are being evaluated for the QCSEE blade under other NASA and related programs.

17. Key Words (Suggested by Author(s))

Composite Blades
Fan Blades
Aerodynamics
Aircraft Propulsion and Power
Variable Pitch Fan

19. Security Classif. (of this report)	20. Security Classif. (of this page)	21. No. of Pages	22. Price*
Unclassified	Unclassified		

FOREWORD

This report was prepared by the Aircraft Engine Group of the General Electric Company, under contract NAS3-18021, for the NASA Lewis Research Center, Cleveland, Ohio. Mr. Morgan Hanson was the NASA UTW Composite Blade Project Manager.

This report covers the preliminary design test effort of the Under-The-Wing (UTW) composite fan blade.

TABLE OF CONTENTS

LIST OF ILLUSTRATIONS

LIST OF ILLUSTRATIONS (Concluded)

LIST OF TABLES

1.0 SUMMARY

This report presents the results of tests conducted on preliminary design polymeric composite fan blades for Under-the-Wing (UTW) QCSEE engine.

The fan blade of composite material incorporates design features gained from previous composite blade programs. This technology is then integrated with a variable pitch mechanism which allows the blade to rotate through both stall and flat pitch conditions.

During this phase of the program a total of 17 preliminary QCSEE UTW composite fan blades were manufactured for various component testing including frequency characteristics, strain distribution, bench fatigue, dovetail pull, whirligig high cycle fatigue, whirligig low cycle fatigue, whirligig strain distribution, whirligig overspeed and whirligig impact. All tests were successfully completed with the exception of the whirligig impact tests. Initial impact test results indicate a deficiency in local impact capability. Improvements in local impact capability are being evaluated for the QCSEE blade under other NASA and related programs.

Blade strength capability in terms of centrifugal and bending loads indicate good margins of safety and provide the necessary data to indicate safe engine operation.

2.0 INTRODUCTION

The Quiet Clean Short-Haul Experimental Engine Program provides for the design, fabrication, and testing of experimental, high-bypass, geared turbofan engines and propulsion systems for short-haul passenger aircraft. The overall objective of the program is to develop the propulsion technology required for future externally blown flap types of aircraft with engines located both under-the-wing and over-the-wing.

This report presents the results of the preliminary design test effort of the under-the-wing composite fan blade.

3.0 DESIGN CONFIGURATION

3.1 BLADE CONFIGURATION

The molded blade configuration consists of a solid composite airfoil and a straight bell-shaped composite dovetail. The dovetail is undercut at the leading and trailing edges to reduce local stresses and to permit better transitioning of the cambered airfoil section into the straight dovetail.

The airfoil definition is described by 15 radially spaced airfoil cross sections which are stacked on a common axis. The dovetail axial centerline is offset from the stacking axis by 0.254 cm (0.1 in.) to provide a smooth airfoil-to-dovetail transition. The molded blade, as shown in Figure 1, is provided with a reduced leading edge thickness to allow a final coating of wire mesh/nickel plate for leading edge protection. The blade leading edge protection is shown on the finished blade drawing (see Figure 2).

A summary of the aero blade parameters is presented in Table I. The low root solidity of 0.98 is required for reverse pitch operation. Except for the large tip chord (high blade flare), the blade length, thickness, and twist dimensions are similar to previous composite blades which have undergone extensive development and proof testing.

3.2 BLADE LAYUP/MATERIAL SELECTION

The material selection and ply arrangement for the UTW hybrid composite blade is based on previous development efforts conducted by General Electric and sponsored by NASA under contract NAS3-16777. This work led to the selection of a combination of fibers in a single blade to provide the proper frequency response and bird impact characteristics to satisfy STOL engine conditions. Figure 3 shows the general arrangement of the plies in the QCSEE UTW composite blade. The flex root surface plies in the lower region of the blade contain S-glass fibers. These plies, being near the surface and having relatively low bending stiffness and high tensile strength, provide higher strain-to-failure characteristics, thereby allowing the blade to absorb large bird-impact loading without the classic root failure that usually accompanies brittle composite materials. Torsional stiffening plies in the airfoil region of the blade are oriented at ± 45° to provide the shear modulus required for a high first torsion frequency. These plies contain boron towards the outer surfaces of the blade and graphite (Hercules AU) in the inner regions.

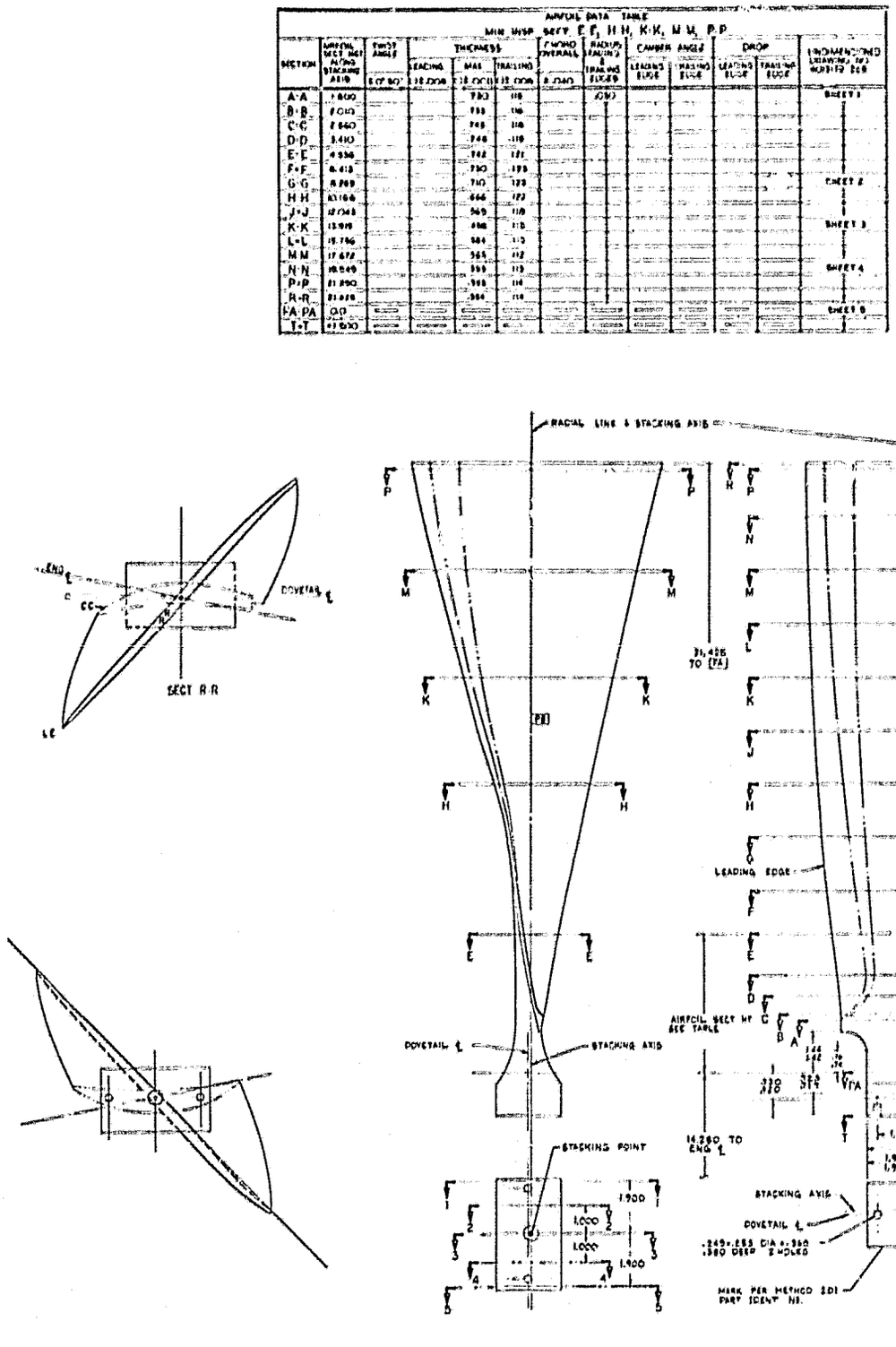

Figure 1. QCSEE Stage One Molded Fan Blade.

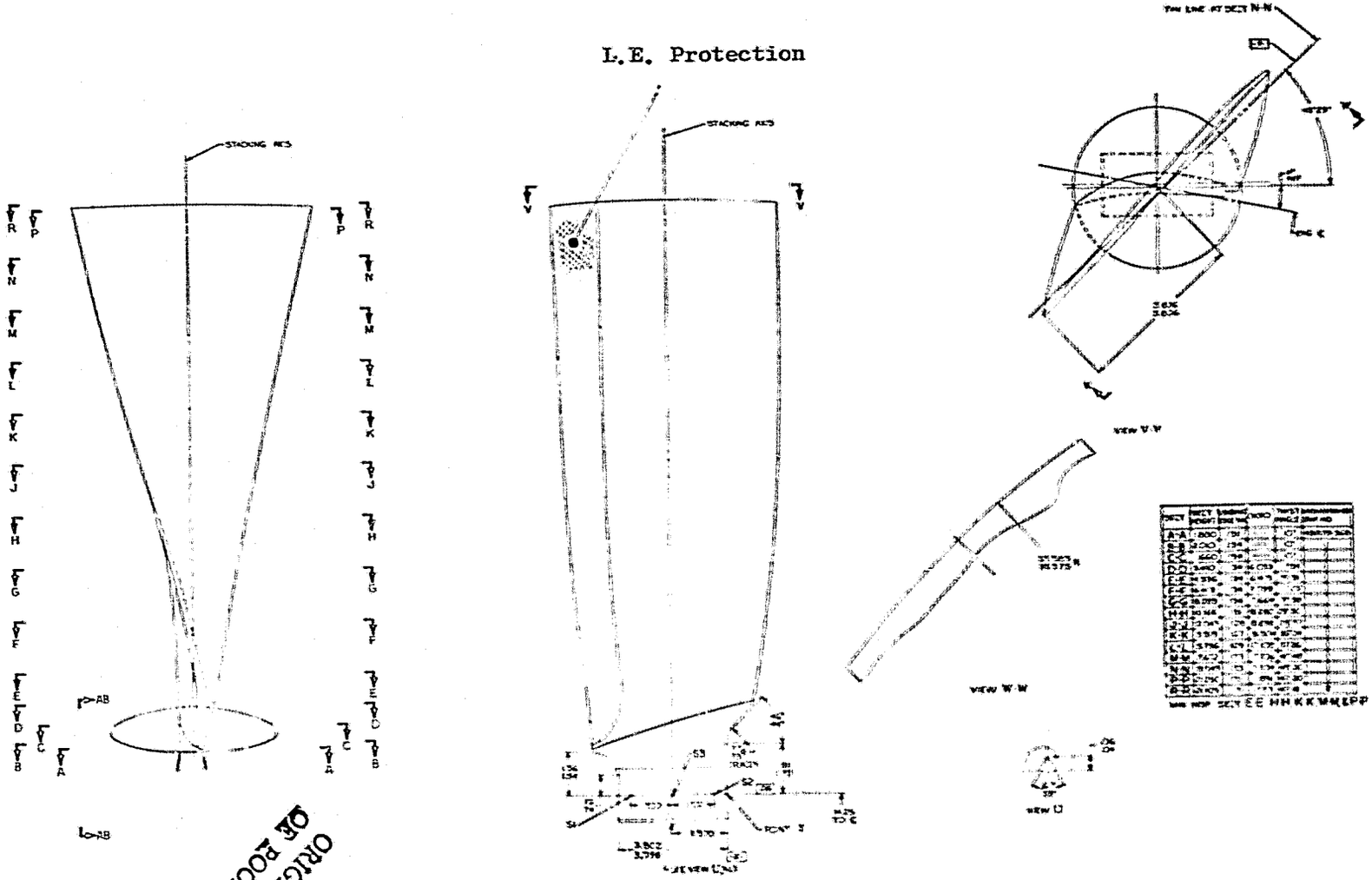

Figure 2. QCSEE Stage One Fan Blade.

Table I. QCSEE - UTW Composite Blade Design Parameters.

Aero Definition	
Tip Speed	306 m/sec (1005 ft/sec)
Tip Diameter	180 cm (71 in.)
Radius Ratio	0.44
Number of Blades	18
Bypass Pressure Ratio	1.27 Takeoff
Aspect Ratio	2.11
Tip Chord	30.3 cm (11.91 in.)
Root Chord	14.8 cm (5.82 in.)
T_M Root	1.93 cm (0.76 in.)
T_M Tip	0.91 cm (0.36 in.)
Root Camber	66.2°
Total Twist	45°
Solidity	
Tip	0.95
Root	0.98
Angle Change from Forward to Reverse	
Through Flat Pitch	75°
Through Stall	100°

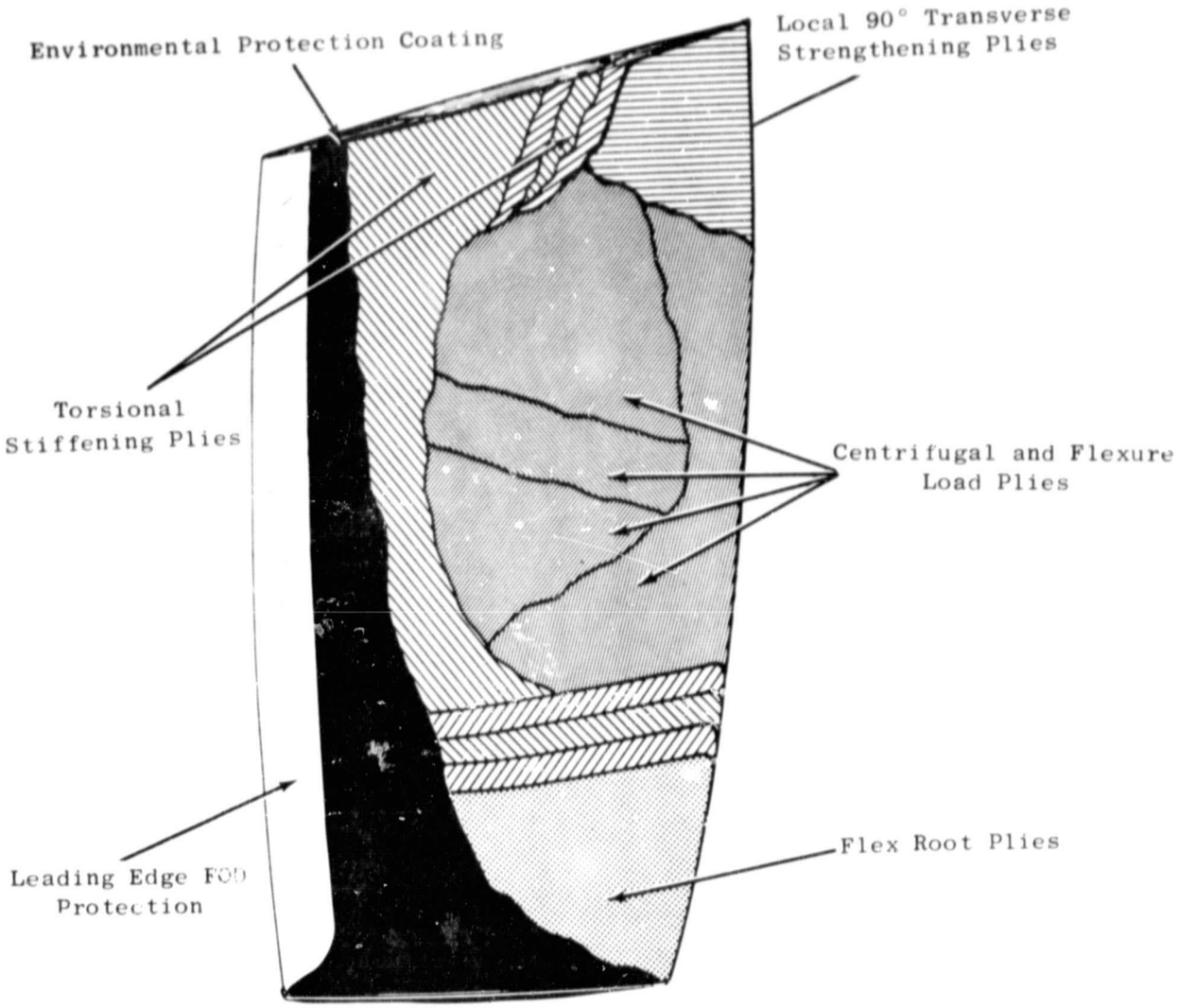

Figure 3. Composite Blade Ply Orientation.

Plies of Kevlar-49 are interspersed throughout the blade with the majority of them being in the longitudinal direction of the blade. Several of the Kevlar-49 plies in the tip region of the blade are oriented at 90° to the longitudinal axis to provide chordwise strength and stiffness to the blade for local impact improvement.

The resin system used in this program is a product of the 3M Company and is designated as PR 288. This is a resin system that has proven satisfactory for the needs of advanced composite blading. Some of its unique characteristics in the prepreg form are:

- has consistent processing characteristics
- can be prepregged with many different fibers including hybrids
- uniform prepreg thickness and resin content

A typical layup (showing one half of the blade) of the Design 1 QCSEE blade is shown in Figure 4.

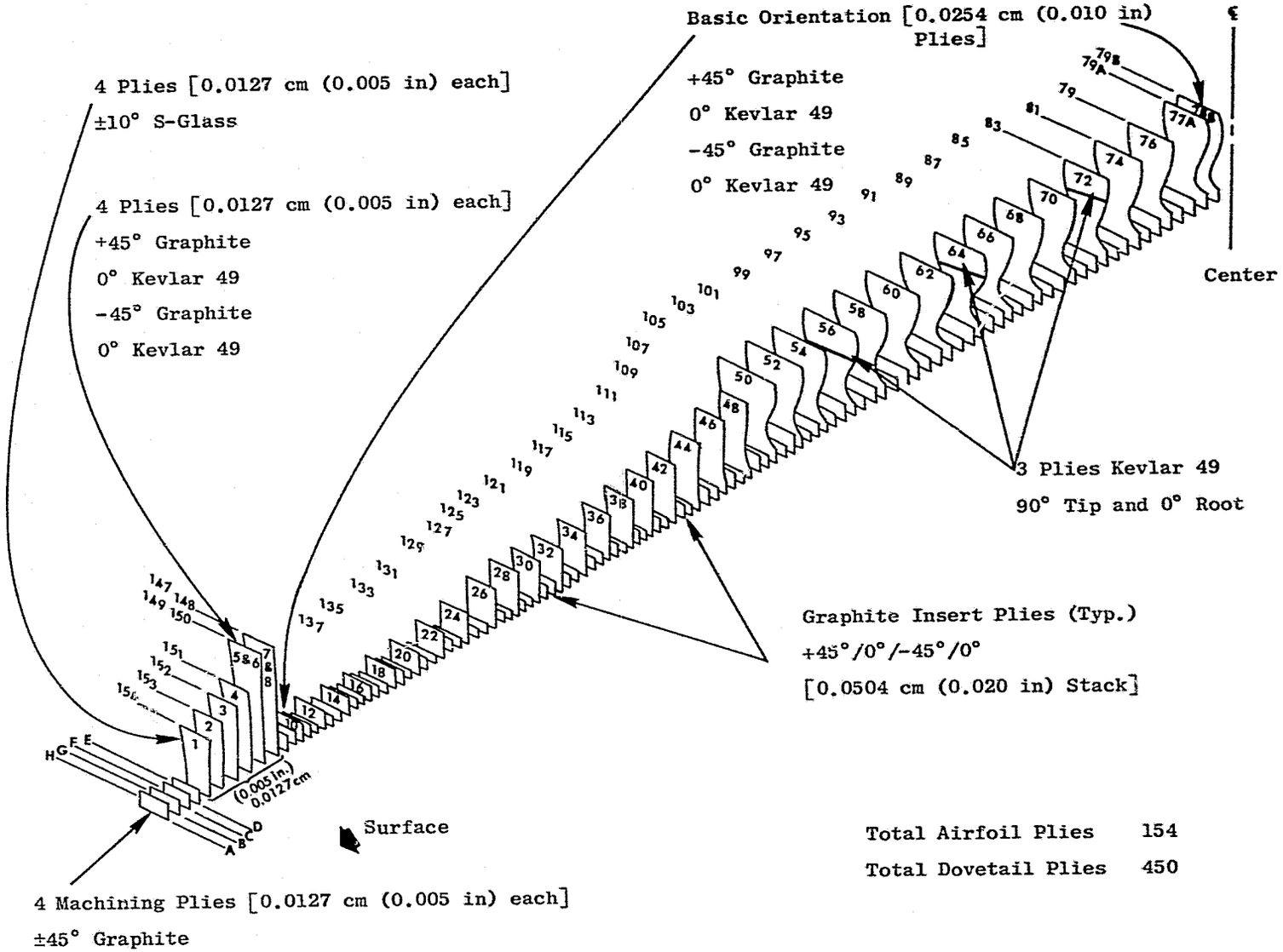

Figure 4. Ply Orientation and Layup (Design I).

4.0 FABRICATION

To assure production of high quality blades, a quality control procedure was established. The following paragraphs describe the methods used to assure the required blade-to-blade consistency. All the materials used were procured to General Electric specifications.

4.1 RAW MATERIAL CONTROL

An established quality control plan for inspecting incoming epoxy prepregs at General Electric was employed on all materials procured under this program. This plan, which establishes the requirements and methods for selecting satisfactory prepreg material for use in composite blade molding activities, includes the following operations:

1. Checking inventory of incoming material and vendor's certifications for completness and reported conformance to specification requirements.

2. Logging in each lot and roll received.

3. Visual inspection of workmanship.

4. Sampling of material and verification of compliance with specification requirements, including physical properties, reactivity, and mechanical properties of a molder panel from each combination of fiber and resin batch.

5. Handling, storage, and reinspection of out-of-date materials.

6. Disposition of materials which fail to meet specification requirements.

Specific material properties which were measured and compared to vendor reported data on each prepreg lot are given below:

Prepreg Data	Laminate Data
Fiber, g/m^2	Flexure str. at RT, 394° K (250° F)
Resin, g/m^2	Flexure mod. at RT, 394° K (250° F)
Solvent content, % wt	Shear str. at RT, 394° K (250° F)
Gel time, minutes at 383° K (230° F)	Fiber content, % vol
Flow, % wt	Resin content % vol
Visual discrepancies	Voids, % vol
	Density, g/cc

4.2 BLADE MOLDING

The basic sequence of operations involved in molding the QCSEE composite blades is outlined below:

1. The fully assembled mold tool was heated to the prescribed temperature in the press such that all sections of the die were maintained at a uniform temperature.

2. The press was opened and release agent was applied to the mold cavity surfaces and any excess removed.

3. The assembled blade preform was loaded into the heated mold cavity.

4. The press closed at a fast approach speed until the top and bottom portions of the mold engaged.

5. An intermediate closing speed was selected for preliminary debulking of the blade preform.

6. The dies continued to close at a preselected, slow rate. The movement continued until the die was closed and the prescribed molding load/pressure attained. Figure 5 shows a typical rate of closure and load application curve for molding a PR 288/Type AU composite blade with a gel time of 60 ± 5 minutes at the constant molding temperature 383° K (230° F).

7. The press was opened and the blade molding was rapidly transferred into the postcure oven, thus preventing thermal contraction stresses from being set up in the part. The blade was allowed to hang freely in the postcure oven for the predetermined process time necessary to achieve full material properties

   Each blade was layed up in halves and weighed prior to molding. Molding temperature was 383° K (230° F). After cooling and deflashing, the blades were weighed and density measurements were taken. Along with the blade, go-by test panels were fabricated concurrently to verify mechanical properties.

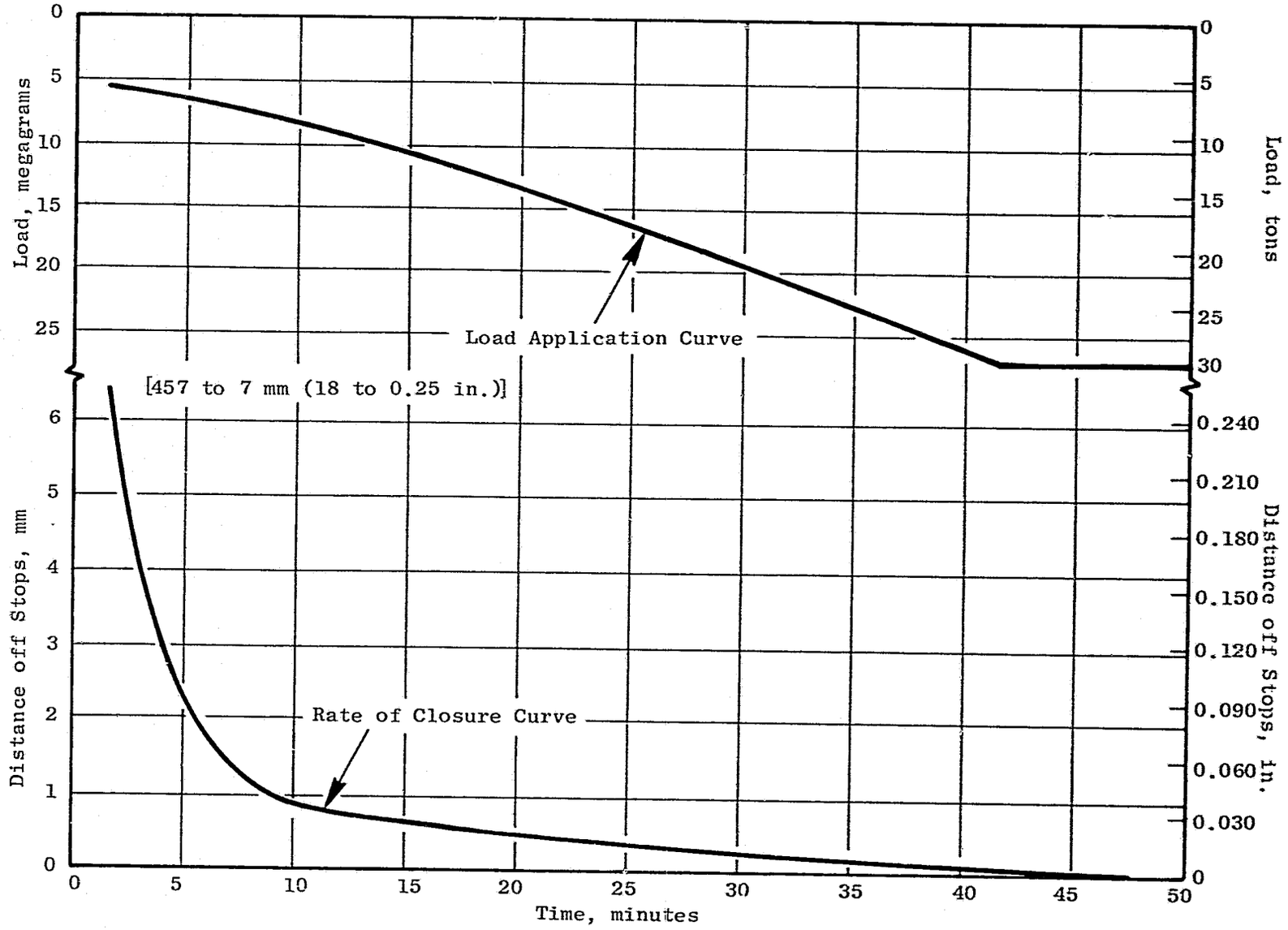

Figure 5. Molding Procedure for PR 288/Type AU Blade with Gel Time at 124° K (230° F).

4.3 MOLDING INSPECTION AND FINISHING OPERATIONS

After removing the blades from the postcure oven and trimming the resin flash, the following inspection operations were carried out:

1. Measurement and recording of molded weight, volume and density.

2. Recording of surface defects in sketch form and by photographs taken of both sides of the blade.

3. Dimensional inspection and recording of the root and tip maximum dimensions.

Although the blade form was molded well within the desired envelope tolerances, it was extremely difficult to mold the dovetail profile to the accuracy required. As a result, dovetail profiles were final machined to size. Foreign object protection systems were also applied to the blade. The principal finishing operations performed on the blades are listed below:

1. Dovetail machining

2. Application of wire mesh to leading edge

3. Application of nickel plating to wise mesh

4. Trimming blade to length and tip forming.

4.4 NONDESTRUCTIVE EVALUTION

All blade specimens were subjected to through-transmission ultrasonic C-scan (TTUCS) inspection before and after testing in addition to holographic and root dye penetrant inspection.

4.4.1 Through-Transmission Ultrasonic C-Scan

The test technique, shown in Figure 6, is basically a measurement of sound attenuation due to both absorption and scattering. The through-transmission approach (as opposed to pure pulse-echo or reflection-plate pulse-echo/transmission approaches) provides for a more efficient energy transfer with a minimal influence of test equipment configuration or material/component shape. The scanner contour follows the airfoil with a master/slave servomechansim. Even so, the attenuation values must be referenced to a specific ply stackup and process sequence employed in the manufacture of each component.

High-resolution scanning (75 lines per inch for 15,000 units of data per square inch), combined with 10 shades-of-gray (5% to 95% on the oscilloscope) recording on dry fascimile paper, provides an "attenugraph" image which is read much in the same manner as a radiograph.

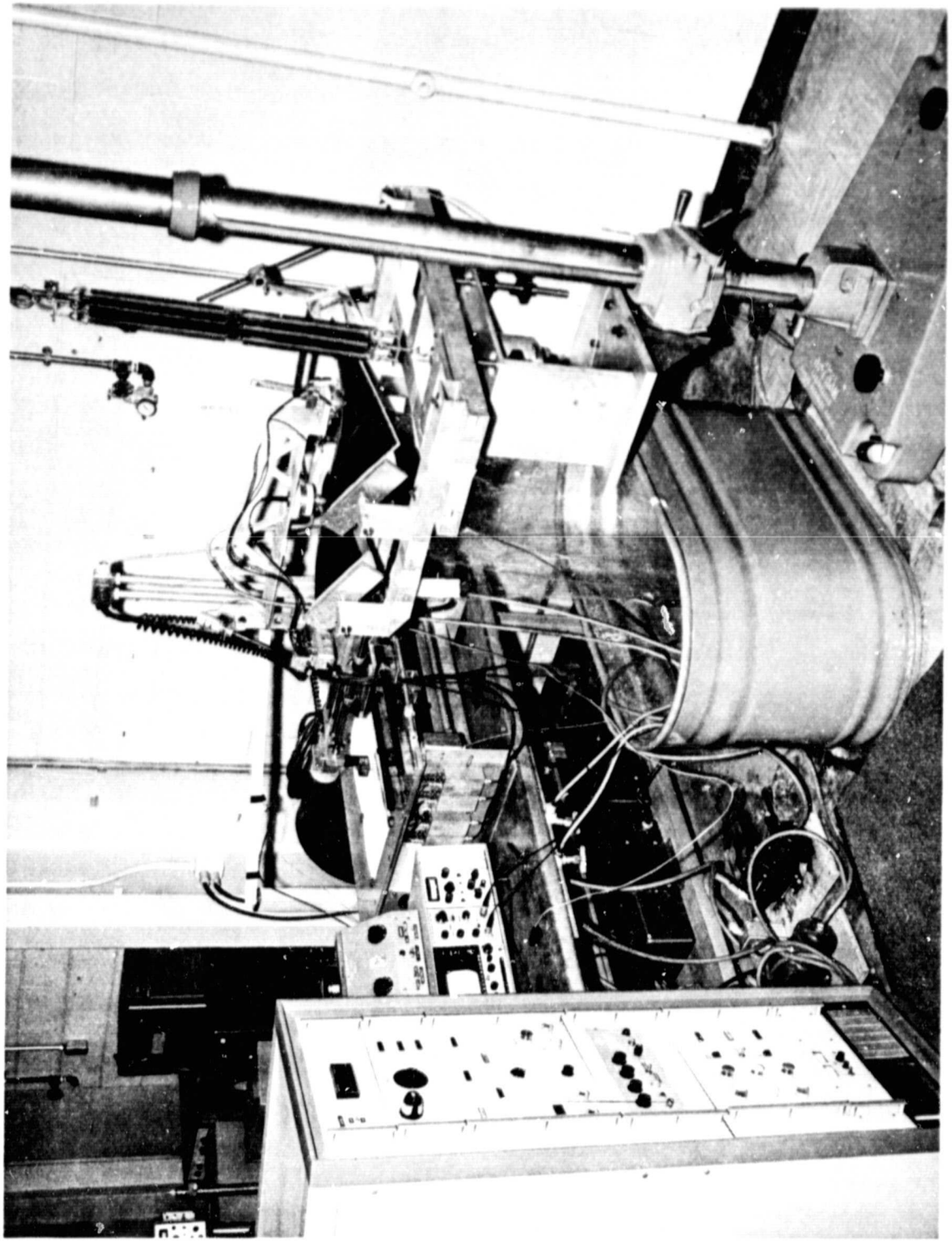

Figure 6. Test Technique for Ultrasonic C-Scan of Composite Blades.

4.4.2 Laser Holographic Interferometry

The laser holographic facility, Figure 7, was also used to inspect the blades molded during this program. It is highly versatile in that the optical devices may be positioned to accomodate a variety of object types and fields of illumination on panels, blades, and other contoured components. Interferometry relies on secure blade fixturing and consistently reproducible stressing for the second exposure of a double-exposure hologram. Typical interferograms are presented in Figure 8.

4.4.3 Dye Penetrant Inspection

Dye penetrant inspection of the dovetail area was performed on each of the blades. This test was used to detect surface-connected root delaminations in the machined dovetail. The dye penetrant check also gives qualitative indications of root zone porosity.

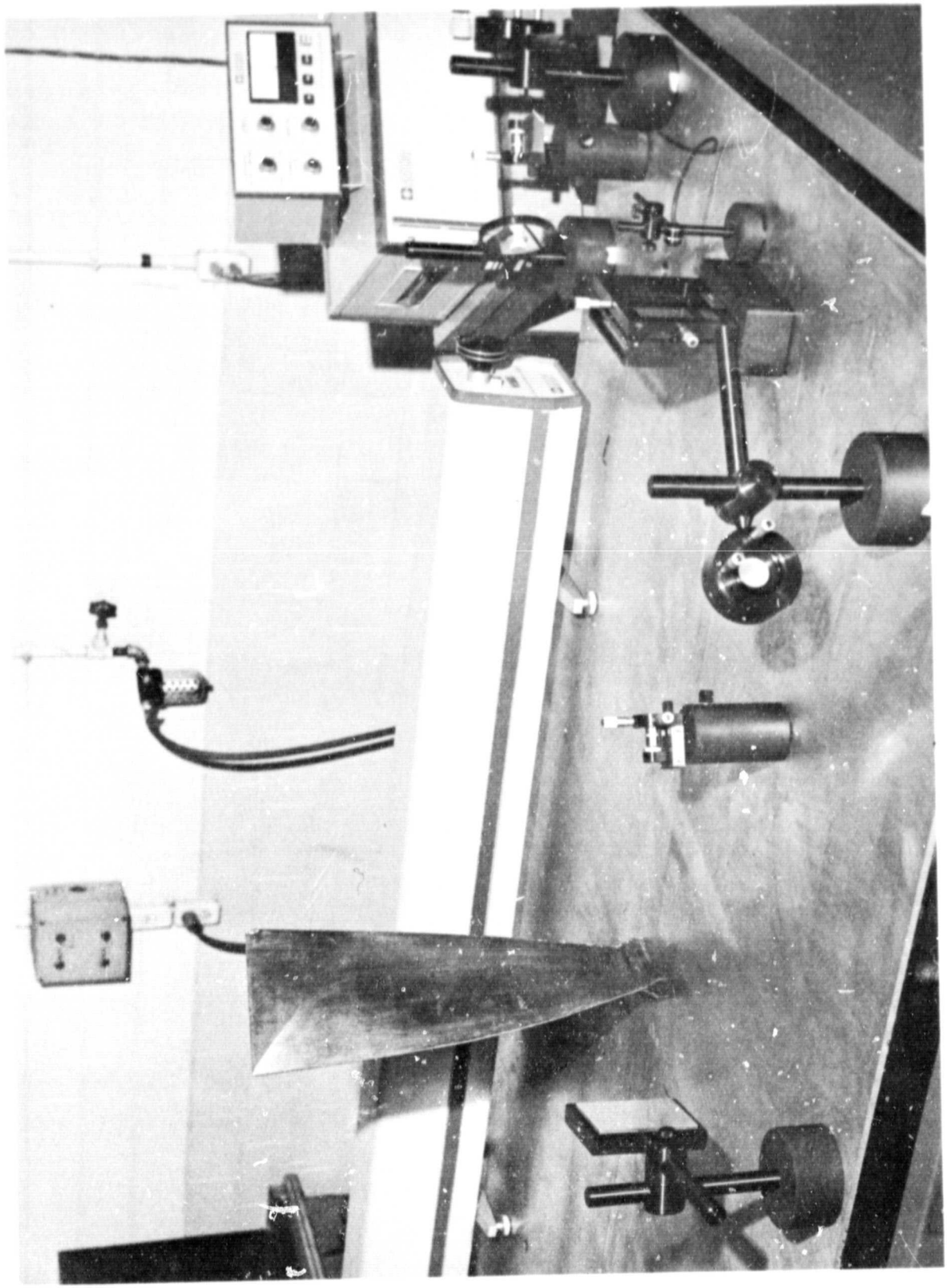

Figure 7. Laser Holographic Facility.

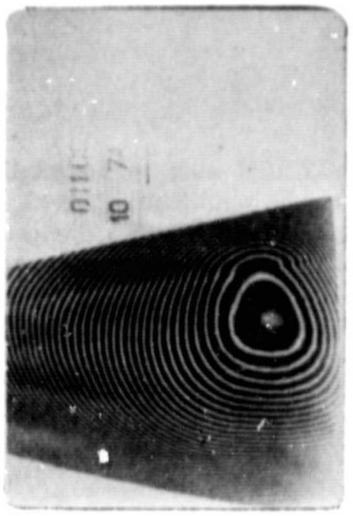

(a) Concave - Tip
No Discontinuity

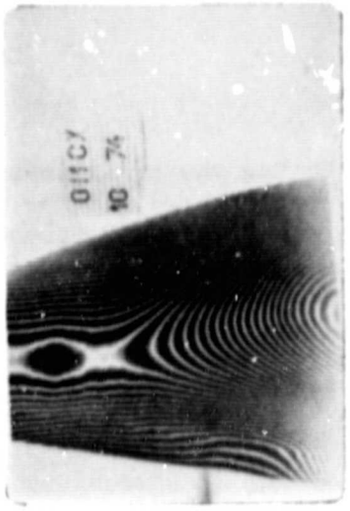

(b) Convex - Tip
No Discontinuity

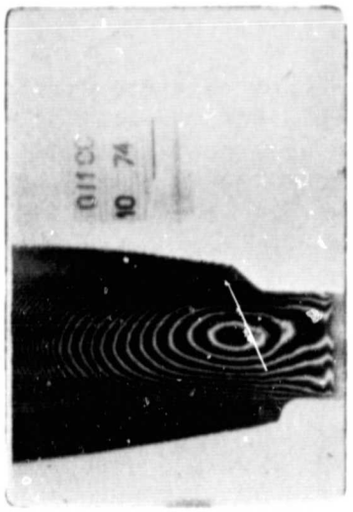

(c) Concave - Root
Slight Discontinuity Due to Ply Slippage

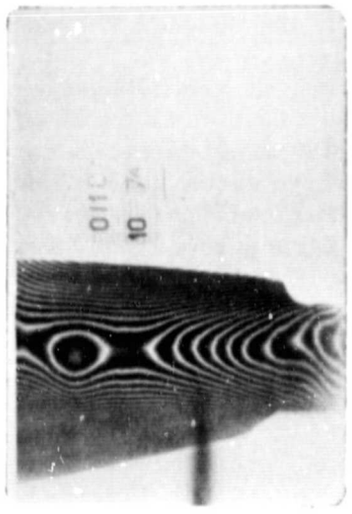

(d) Convex - Root
No Discontinuity

Figure 8. Holograph NDT of QCSEE Blade.

5.0 UTW COMPOSITE BLADE TESTING

During the preliminary design phase, a total of 17 UTW composite blades were manufactured for the purpose of evaluating the blade mechanical design to determine blade frequency characteristics, strength, and impact capability. The 17 blades were manufactured using 6 hybrid material configurations including Kevlar-49/Boron (3), Kevlar-49/Graphite (1), Kevlar-49/Graphite/Boron (9), Kevlar-49/AU Graphite/HM Graphite (1), S-Glass/Hybrid Graphite/Boron (2), and Kevlar-49/Hybrid Graphite (1). The majority of the blades were manufactured in the final material configuration of Kevlar-49/Graphite/Boron.

Of the 17 blades eight were used for bench and whirligig testing according to the test plan shown in Table II.

Whirligig testing is described in Section 6 of this report. Bench testing and results are given as follows:

5.1 BLADE FREQUENCY CHARACTERISTICS

All of the 17 blades manufactured underwent frequency characterization in the first five modes of vibration. A summary of this data as well as the corresponding material configuration of each blade is presented in Table III. This data shows good blade-to-blade consistency of the selected blade material configuration. The 1F, 2F and 1T frequencies are acceptable for meeting aeromechanical requirements.

5.2 DOVETAIL PULL TESTS

The successful operation of composite blades under engine operating conditions depends to a great degree on the load carrying capability of the dovetail attachment. For this reason, two blades, S/N QP002 and QP003 were subjected to tensile load in a manner as shown in Figure 9. The purpose of these tests was to determine the ultimate strength of the dovetail of two blade materials, the first and succeeding load points where audible indications of fiber breakage occurs, and the mode of failure when it occurs.

The test assembly is shown in Figure 10. Each blade was loaded in the radial direction through the stacking axis in increments consisting of 22.2 kN (5000 lb) steps to 222 kN (50,000 lb) and then 8.9 kN (2000 lb) steps to termination.

The root of each blade was strain gaged as shown in Figure 11. Strain readings were recorded at each load point, audible indications were noted in the test log when they occurred, and visual observations for damage such as fiber breakage or delamination were made.

Table II. Composite Blade Test Plan.

Test	Blade S/N	Material Combination	Planned Testing
1. Dovetail Pull	QP002 QP003	Boron/Kevlar-49 Graphite/Kevlar-49	Pull to failure.
2. Bench Strain Distribution	QP007	Boron/Kevlar-49/Graphite	Relative stress at 1st four modes.
3. Bench Fatigue • 1st Flex	QP006	Boron/Kevlar-49/Graphite	10^6 cycles at 276 MN/m^2 (40 ksi), 345 MN/m^2 (50 ksi) etc., double amplitude stress to 5% frequency drop.
4. Whirligig Strain Distribution	QP004	Boron/Kevlar-49/Graphite	Stress distribution at 1st three modes.
LCF	QP004	Boron/Kevlar-49/Graphite	1000 Cycles, 600 to 3500 rpm.
5. Overspeed	QP004	Boron/Kevlar-49/Graphite	5 minute @ 3800 rpm (115% design speed).
6. Whirligig HCF (1st Flex)	QP008	Boron/Kevlar-49/Graphite	10^6 cycles at 207 MN/m^2 (30 ksi), 276 MN/m^2 (40 ksi) etc., double amplitude stress to 10% frequency drop.
Whirligig HCF (1st Tors.)	QP004	Boron/Kevlar-49/Graphite	5 X 10^6 cycles at 207 MN/m^2 (30 ksi), 276 MN/m^2 (40 ksi), etc., double amplitude stress to 10% frequency drop.
7. Whirligig Impact			Bird Size/ Slice Size kg/kg (oz/oz) / Flight Condition / Blade Span Location,% / Incidence Angle / Rotor Speed rpm
	QP005	Boron/Kevlar-49	.9/.3 32/12 T.O. 80 33° 3360
	QP011	Boron/Kevlar-49/Graphite	.9/.3 32/12 T.O. 80 33° 3250

Table III. Blade Material Composition and Frequency Inspection.

S/N	Surface Plies .013 cm (.005 in.)	0° Plies .025 cm (.010 in.)	±45° Plies .025 cm (.010 in.)	Dovetail Inserts .051 cm (.020 in.)	Frequency – Zero Speed, Hertz				
					1F[a]	2F	1T[b]	3F	2T
QP001	4 – S.G.	18 – Kevlar-49	19 – 80AU/20S.G.	80AU/20S.G.					
QP002	4 – S.G.	18 – Kevlar-49	19 – Boron	S.G.	68	188	292	418	634
QP003	4 – S.G.	18 – Kevlar-49	19 – AU	AU	62	186	257	416	550
QP004	3 – S.G.	18 – Kevlar-49	10 – AU; 9 – Boron	AU	70	202	290	442	610
QP005	3 – S.G.	18 – Kevlar-49	8 – Kevlar-49 11 – Boron	S.G.	68	200	294	438	600
QP006	3 – S.G.	17 – Kevlar-49	14 – AU; 6 – Boron	AU	62	190	288	425	667
QP007	3 – S.G.	17 – Kevlar-49	14 – AU; 6 – Boron	AU	66	192	288	427	666
QP008	3 – S.G.	17 – Kevlar-49	14 – AU; 6 – Boron	AU	61	190	286	438	662
QP009	3 – S.G.	17 – Kevlar-49	14 – AU; 6 – Boron	AU	64	190	284	–	666
QP010	3 – S.G.	17 – Kevlar-49	14 – AU; 6 – Boron	AU	58	190	285	430	672
QP011	3 – S.G.	17 – Kevlar-49	14 – AU; 6 – Boron	AU	56	190	288	424	664
QP012	3 – S.G.	18 – Kevlar-49	8 – Kevlar-49 11 – Boron	S.G.	67	191	286	–	594
QP013	3 – S.G.	17 – Kevlar-49	14 – AU; 6 – Boron	AU	62	190	284	420	662
QP014	3 – S.G.	17 – Kevlar-49	14 – AU; 6 – Boron	AU	67	190	284	424	664
QP015	3 – S.G.	17 – Kevlar-49	14 – AU; 6 – HM	AU	56	178	286	370	686
QP016	3 – S.G.	5 – S.G.; 12 – 80 AU/ 20 Kevlar-49	14 – 80 AU/20 S.G. @ 22° 6 – Boron	S.G.	69	208	292	450	618
QP017	3 – S.G.	5 – S.G.; 12 – 80 AU/ 20 S.G.	14 – 80 AU/ 20 S.G. @ 22° 6 – Boron	S.G.					

(a) Flexural mode
(b) Torsional mode

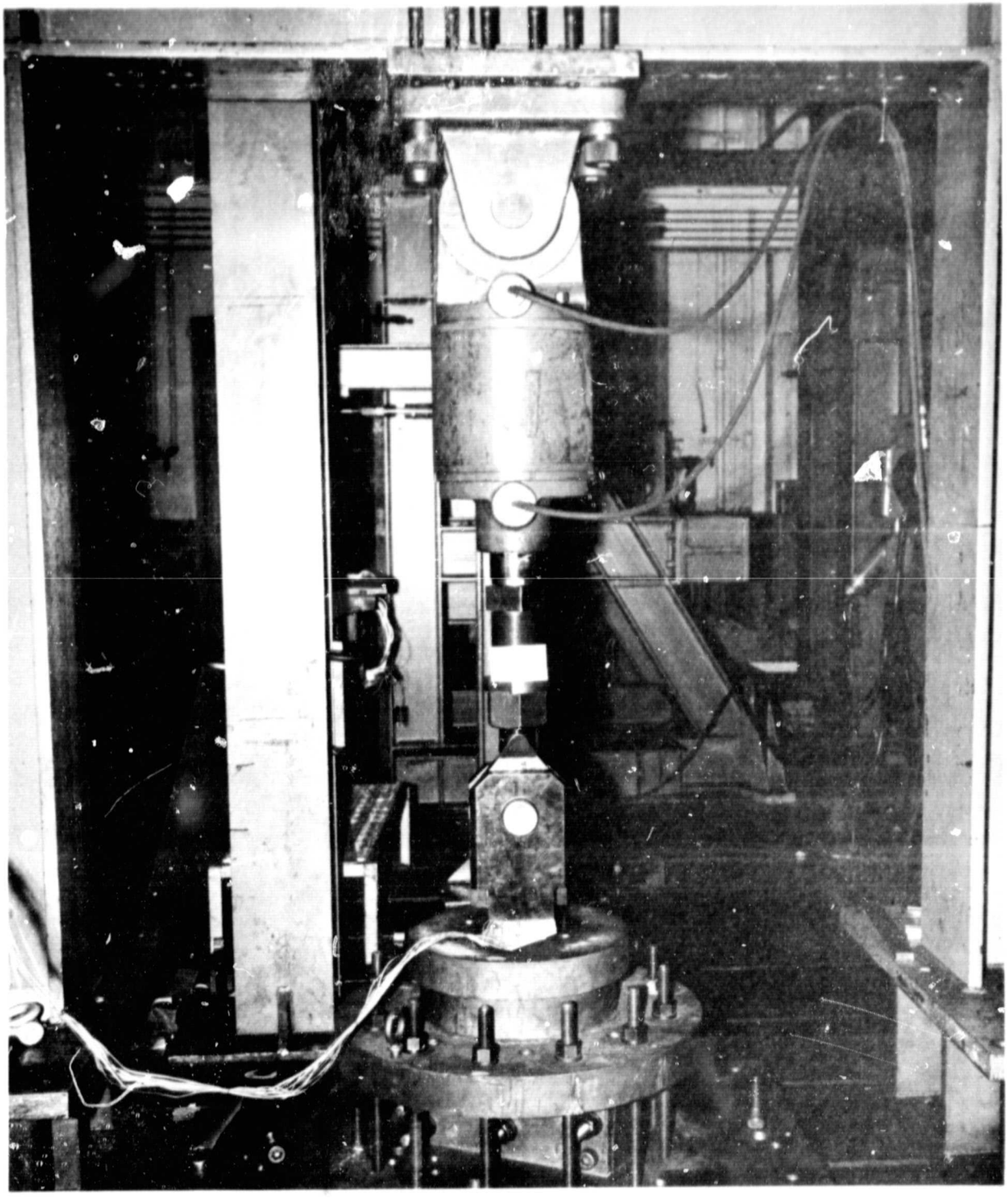

Figure 9. Dovetail Pull Test Setup

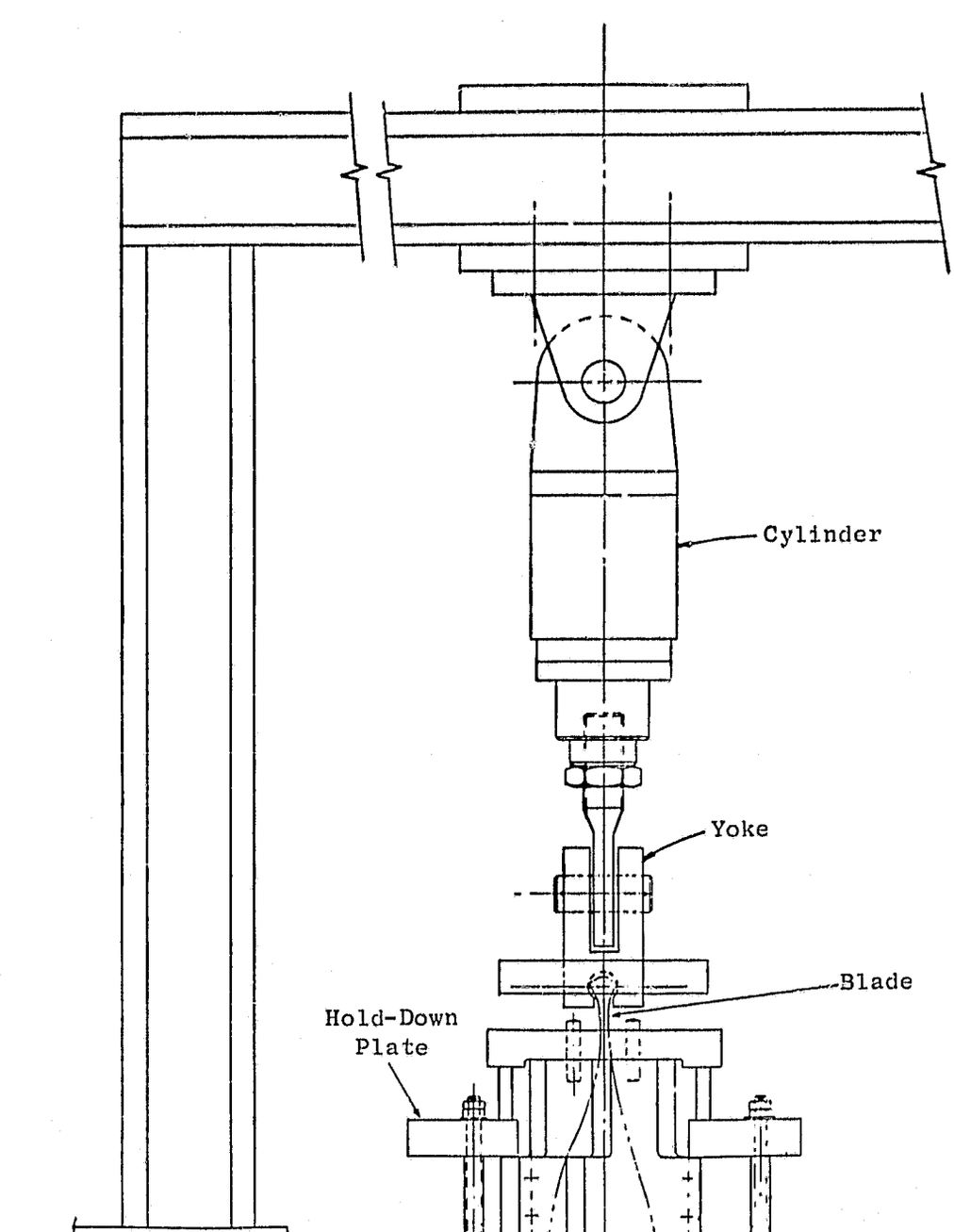

Figure 10. Dovetail Pull Test Assembly.

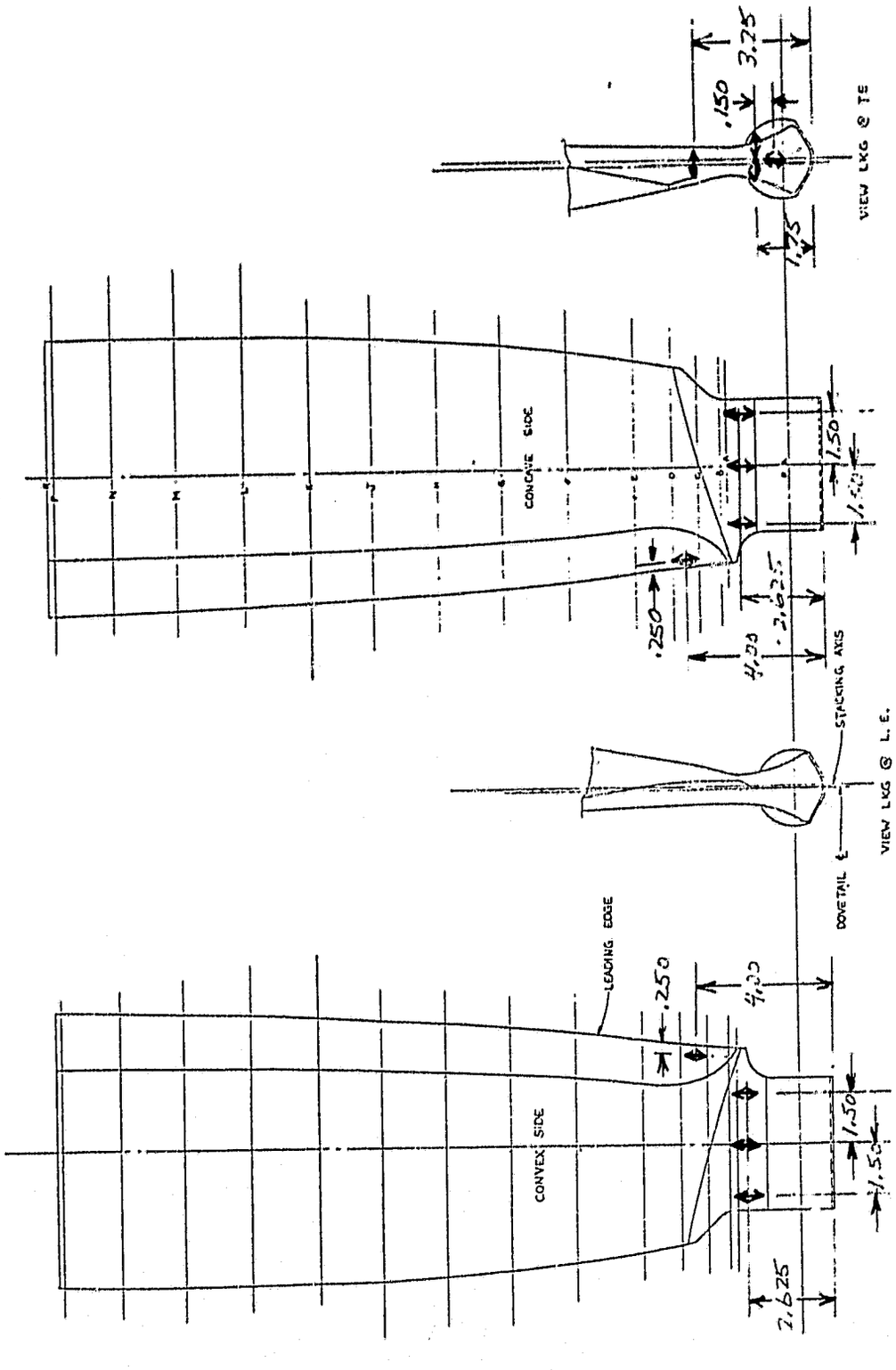

Figure 11. Dovetail Pull Test Strain Gage Locations.

Neither blade dovetail could be loaded to failure as in each case the airfoil pulled loose from the Devcon potting compound and clamping bolts, terminating the test at that point. The maximum load achieved on blade QP002 (Boron/Kevlar-49 material) was 6.58.3 kN (148,000 lb) and on blade QP003 (Graphite/Kevlar-49 material) was 676 kN (152,000 lb). The two blades tested had first audibles at 443 kN (95,000 lb) and 311 kN (70,000 lb) respectively, as evidenced by test monitoring and changes in the strain rate. A typical plot of strain versus load for an instrumented location on the blade is presented in Figure 12 for the QP002 and Figure 13 for blade QP003. This data shows fairly linear strain response up to the first audible where some form of delamination occurs.

Audible and projected ultimate strength levels are well above design load levels indicating approximately 2 to 1 strength to load margins.

The test was halted on blade QP003 after a load of 266.9 kN (60,000 lb) was achieved to examine the 2024-T3 aluminum outsert. The outsert showed very slight indentation of 0.005 to 0.008 cm (0.002 to 0.003 inches) on the external pressure face. No dovetail damage was seen at this point.

Figures 14 and 15 show blade S/N QP002 after it was removed from the test setup. Dye penetrant and ultrasonic C-Scan inspection was performed on each blade and is reported in Figure 16 and 17. The lines and shaded areas represent delaminations in the blade.

5.3 BENCH STRAIN DISTRIBUTION

A bench strain distribution test was performed on blade QP007 for the purpose of determining the areas of strain concentration in the first five natural modes of vibration. This data is useful in assessing relative vibratory stresses of the blade in conjunction with engine testing. Areas of maximum vibratory stress are combined with steady state stresses as a basis for establishing engine operating stress limits.

The strain distribution test was run using an electromagnetic excitation system to excite the blade at a constant force, on resonance, while strain gage readouts were recorded on an HP2010C Data Acquisition System. A diagram of this setup is shown in Figure 18. The blade was instrumented with 200 strain gages, located as shown in Figure 19. The numbered elements in this figure indicate gage locations used for comparative purposes to data obtained from whirligig testing. During the test excitation loading was controlled to provide a strain between 254 and 1270 μcm/cm (100 and 500 μin./in.) at the maximum strain location to assure that no change occurred in the blade or gaging during testing and strains at all other gage locations were recorded as a percentage of the strain at the maximum strain location.

Table IV summarizes this data for the first three natural frequencies along with pertinent data from bench and whirligig fatigue testing. The data shows that in the first flex mode the maximum strain location is the

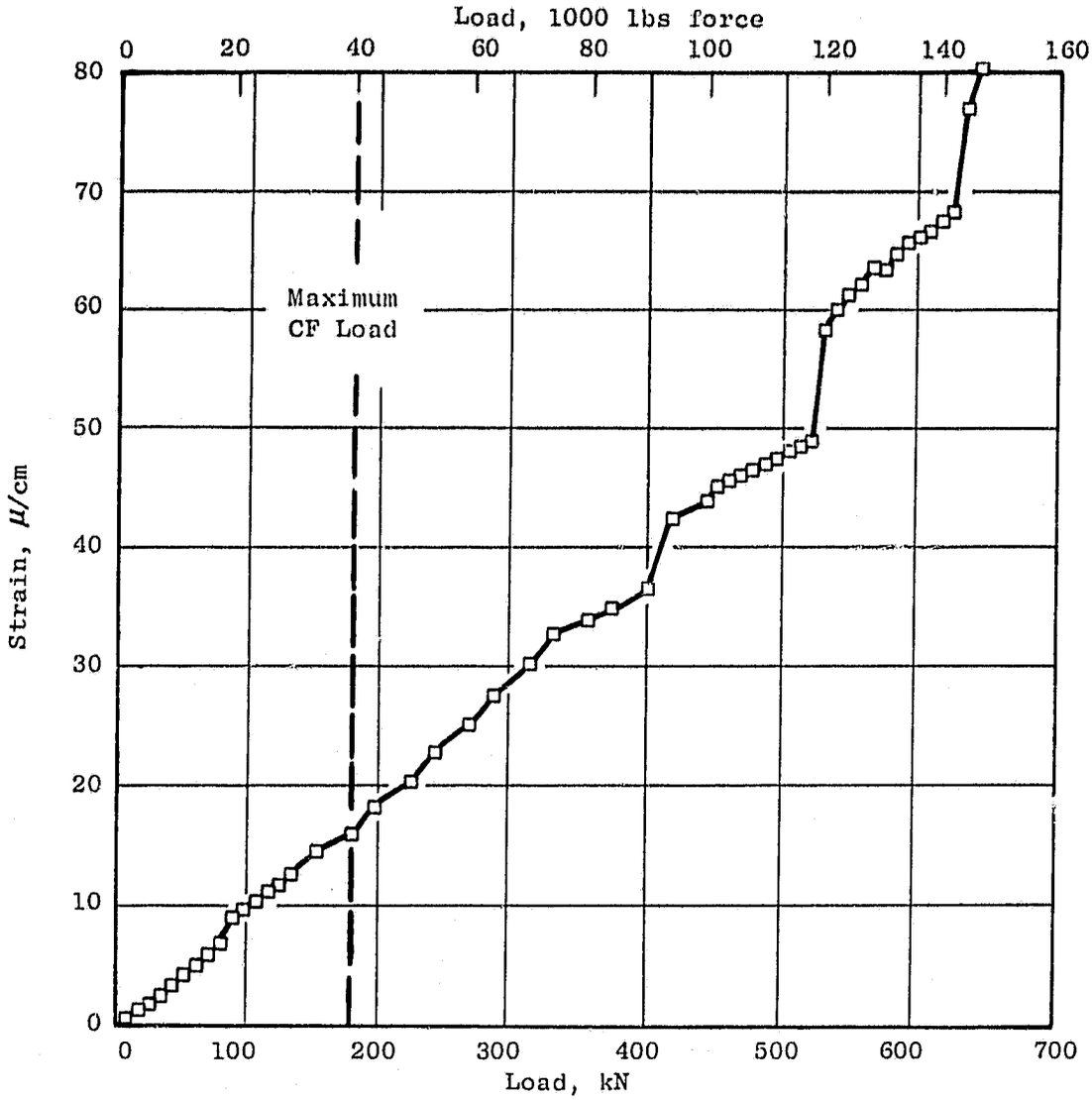

Figure 12. Strain Gage Reading Vs. Applied Load; Blade S/N QP002.

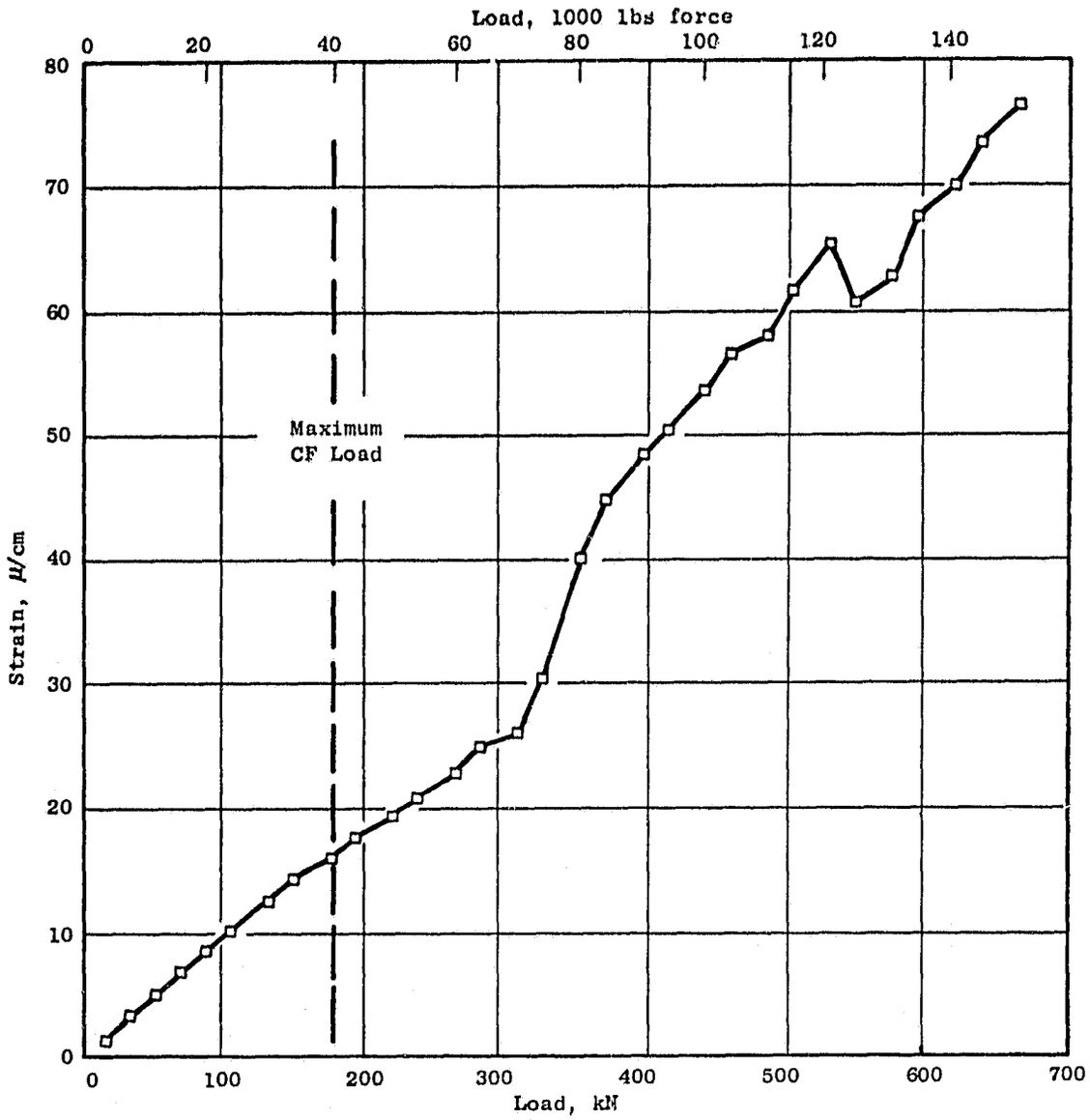

Figure 13. Strain Gage Reading Vs. Applied Load; Blade S/N QP003.

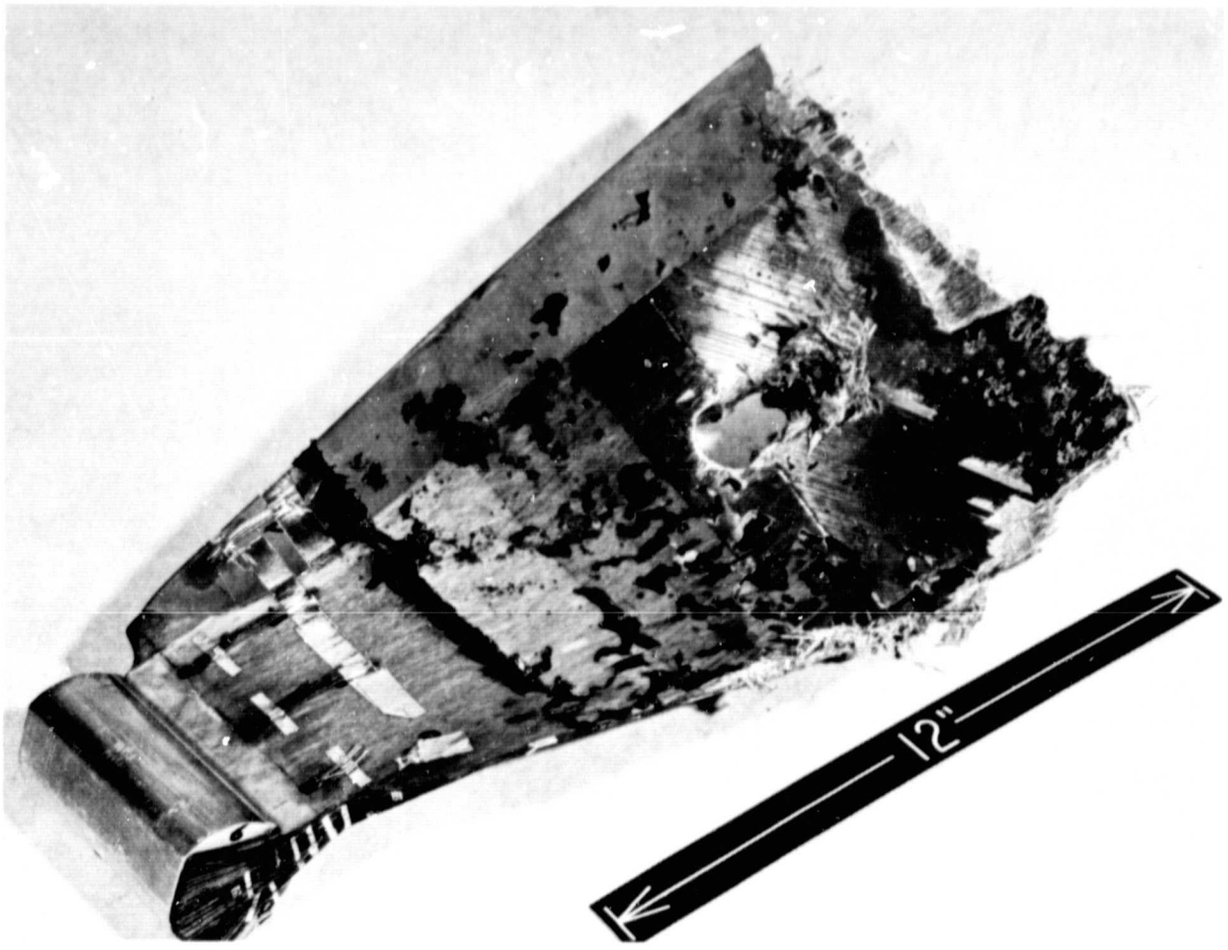

Figure 14. Convex Side of Blade Following Pull Test.

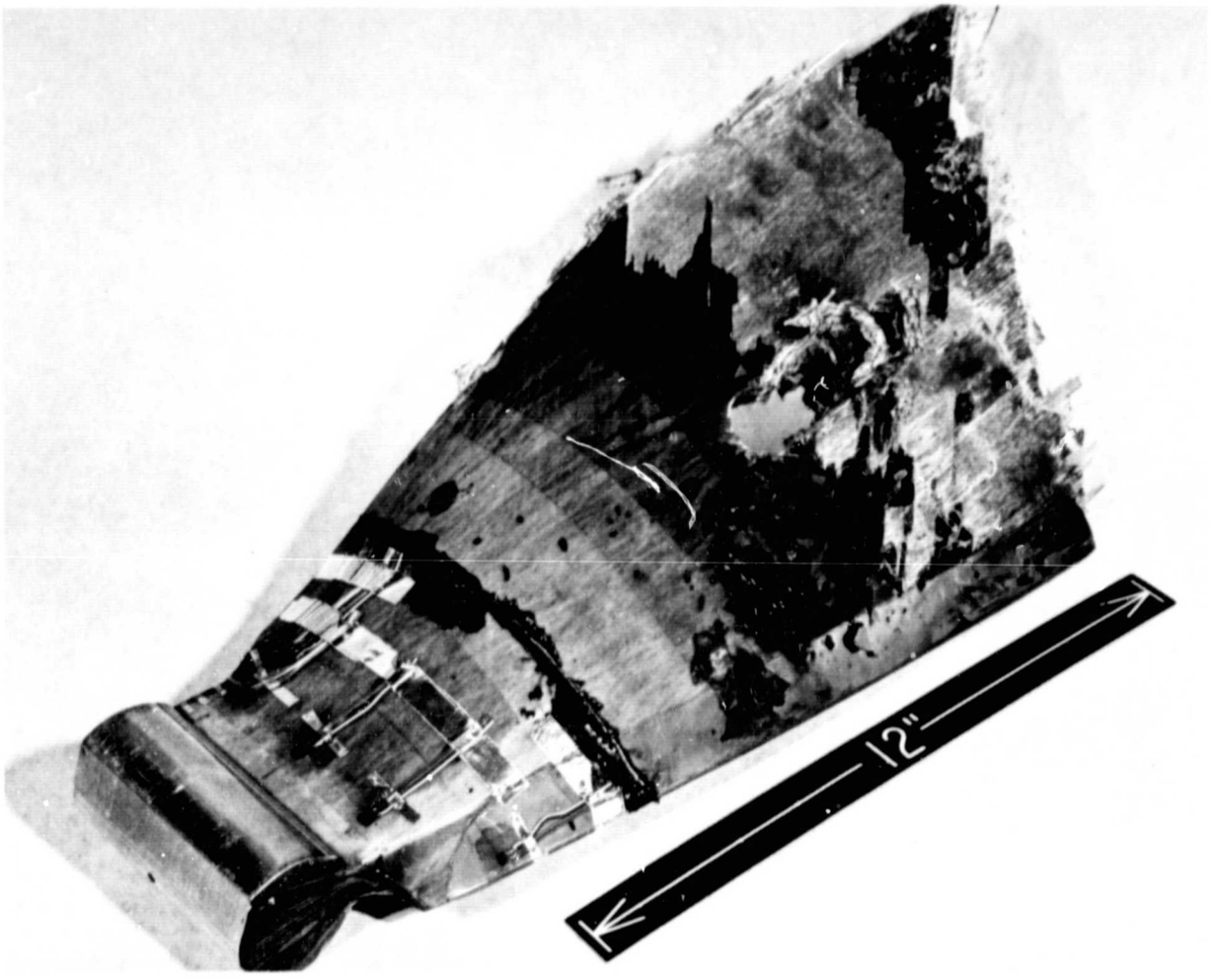

Figure 15. Concave Side of Blade Following Pull Test.

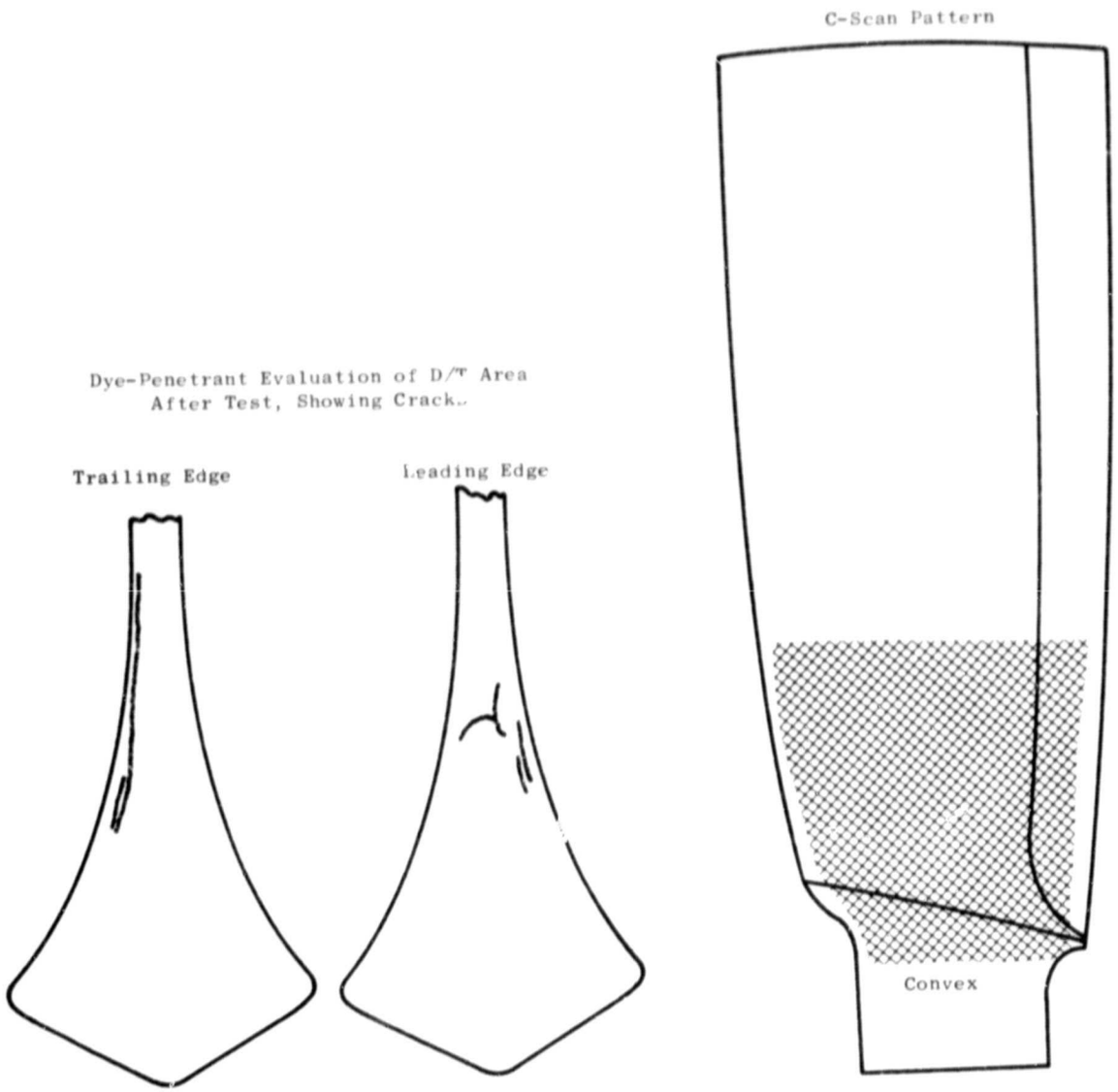

Figure 16. Posttest Inspection of Blade QP002.

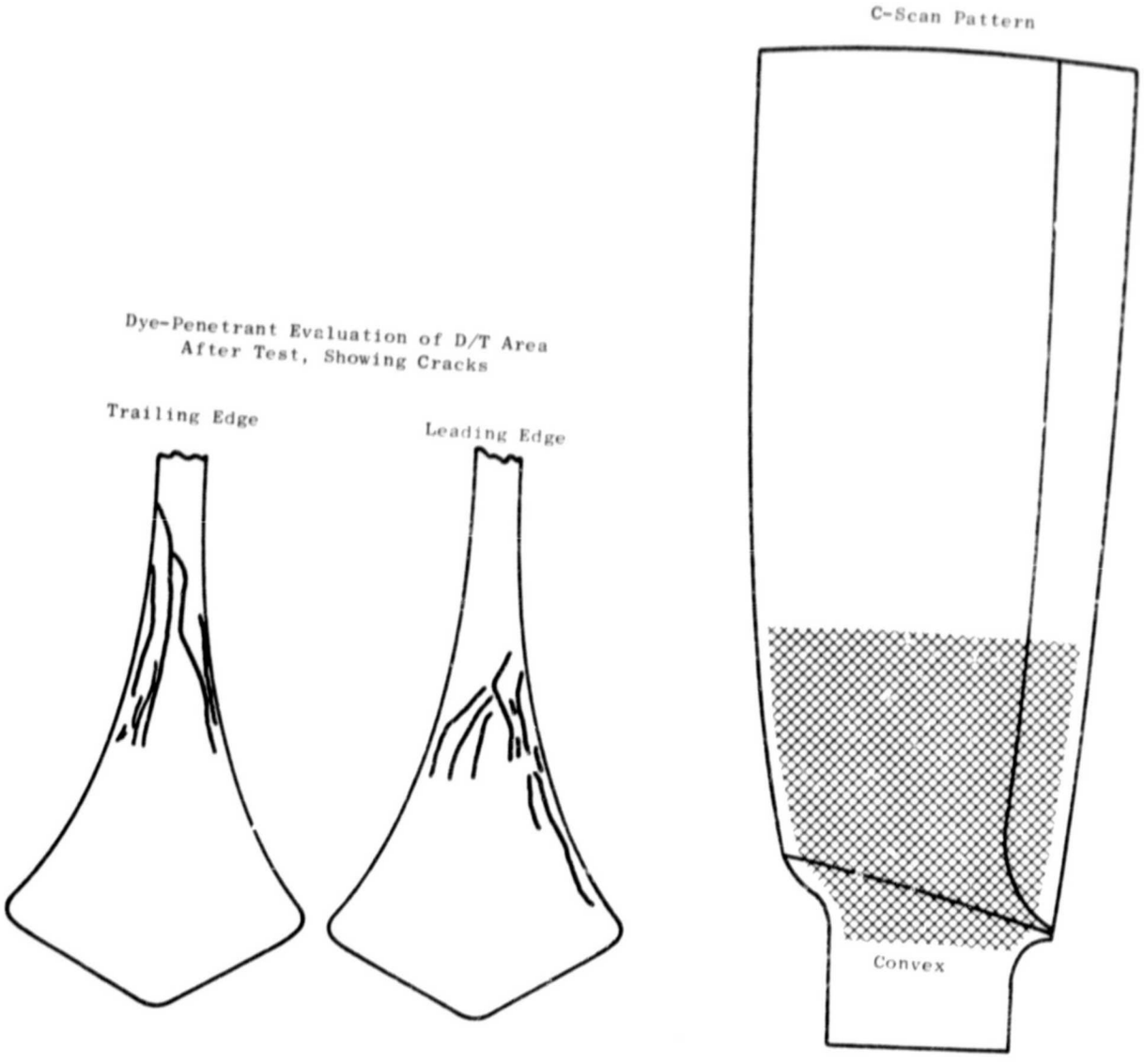

Figure 17. Posttest Inspection of Blade QP003.

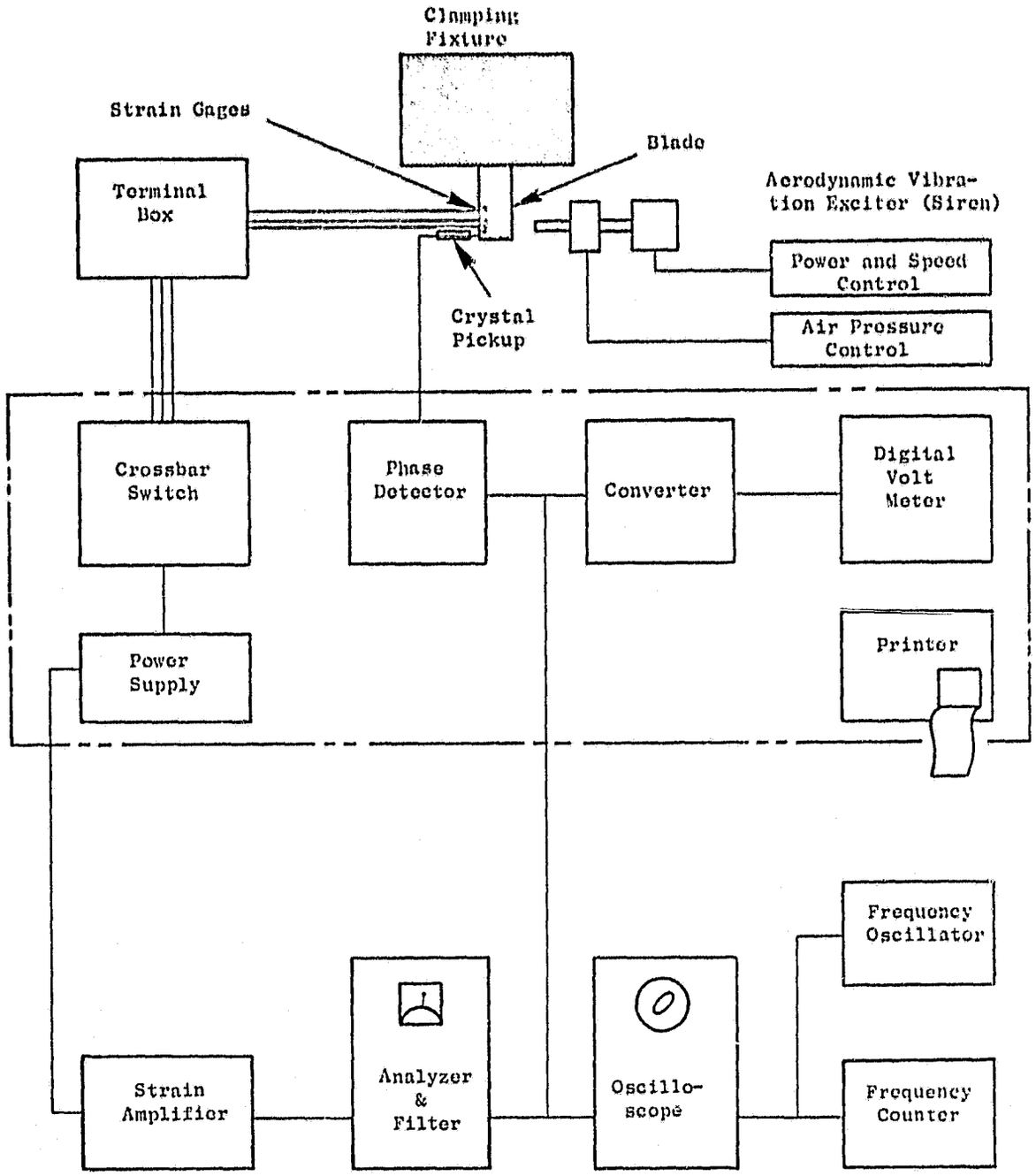

Figure 18. Automatic System for Determining Relative Stress Distribution.

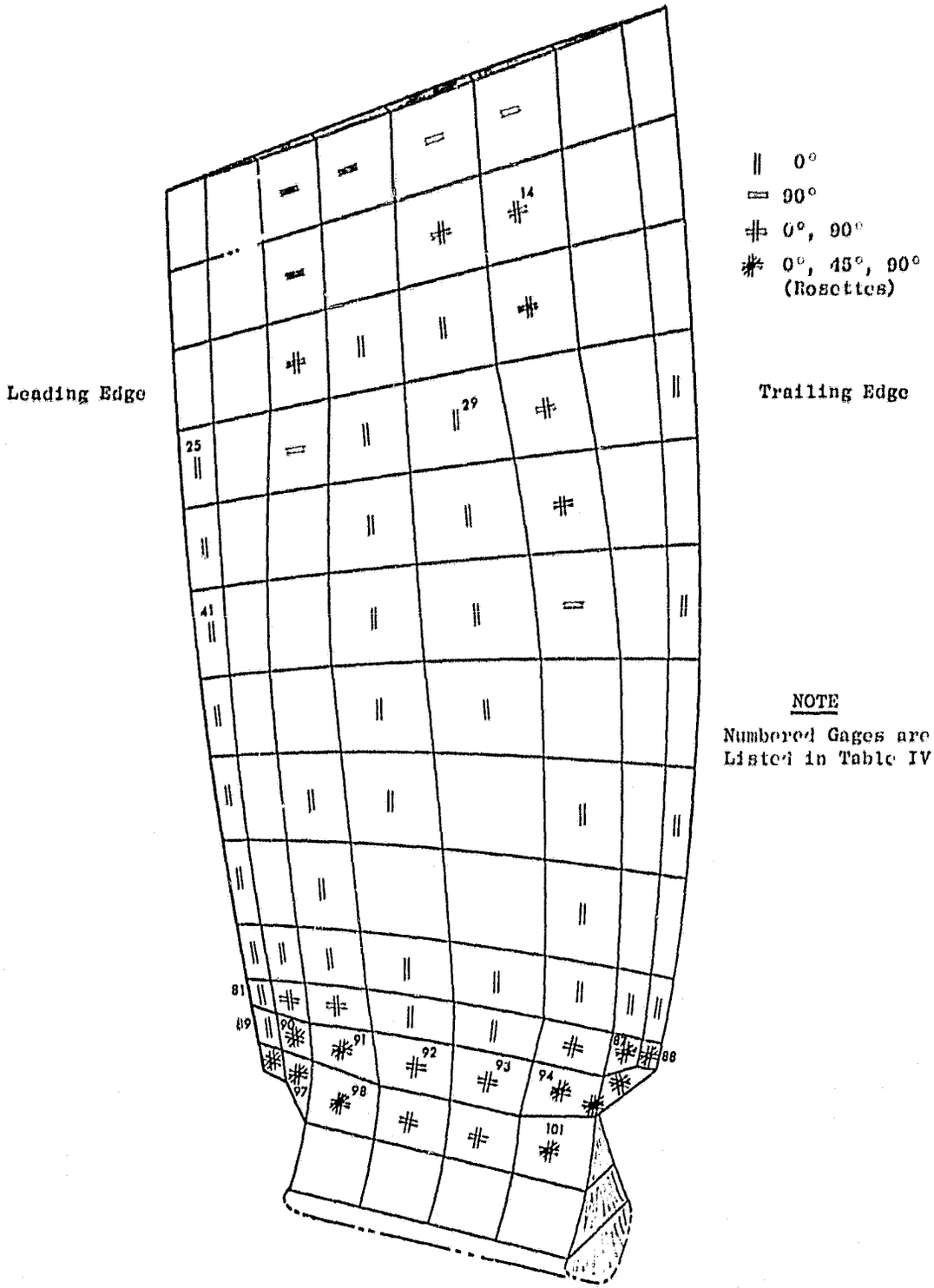

Figure 19. Strain Gage Locations for Bench Distribution Test.

Table IV. Strain Distribution; QCSEE Composite Blade Tests.

• Relative Dynamic Strain

Bench Strain Distribution (QP007)				Whirligig Strain Distribution (QP004)				Bench Fatigue (QP006)	
Gage No.	1F	2F	1T	Gage No.	1F	2F	1T	Gage No.	1F
98	71	100	47	98		100	81	98	66
97	59	81	34	97	61	23	19	–	
89	40	39	9	89	Dut			89	54
90	83	92	8	–				90	77
91	83	100	30	91	63	60	48	–	
101	84	49	68	101	65	83	100	101	78
94-90°	82	52	40	–				94-90°	100
94-45°	25	27	92	–				94-45°	28
94-0°	36	12	28	–				94-0°	51
81	58	52	15	81	38	43	31	81	54
87	46	34	34	87		28	36	–	
88	25	26	29	88	23	30	10	99	13
41	26	36	48	41	13	16	23	–	
25	15	45	73	25	8	36	56	–	
14	8	17	15	14	9	30	15	–	
93	95	90	16	93	96	26	20	93	67
92	100	66	5	92	100	75	44	92	70
41	9	6	58	41	10	30	65	–	
29	29	73	50	29	29	75	55	–	

convex hi-C root region. Secondary regions of high strain are located near the root leading edge and trailing edge undercut on the concave side. In the second flex mode the maximum strain locations are the leading edge root undercut. Maximum strain locations in the first torsion mode are located at the 75% span trailing edge concave side and the root trailing edge undercut region.

5.4 BENCH FATIGUE TEST

A bench high cycle fatigue test was performed on blade QP006 to determine the alternating stress capabilities of the QCSEE blade. This test was performed by clamping the blade dovetail in a holding fixture which is rigidly attached to a table, and exciting the blade in its first flexural frequency. Excitation was provided by a siren facility which produces pulses of air that are directed at the blade. The frequency and magnitude of the pulsating force is regulated until the desired resonant frequency is in its natural mode.

The objective of the fatigue testing was to identify the runout fatigue strength with no frequency drop and also to identify the stress level and number of cycles corresponding to a 10% frequency drop. The blade was instrumented with eight single-element and one three-element rosette strain gages. Gages were placed on the center of selected elements used for the TAMP model with one of the gages placed at the center of the most highly stressed element. Tip deflection and strain gages were monitored while the blade was being excited to fatigue or until the desired number of cycles were reached. Maximum tip deflection was maintained constant during actual cycling because strain gages limited life during cyclic testing. The initial peak double amplitude stress was set at 276 MN/m^2 (40 ksi DA) at the maximum stress location. Runout was considered to be one million cycles. Double amplitude stress increases of 69 MN/m^2 (10 ksi) were used for the subsequent level and testing continued until blade failure resulted. A 10% drop in blade frequency was considered to constitute blade failure.

Fatigue test in the first flexural mode of blade QP006 show these results:

- 10^6 cycles at 276 MN/m^2 (40 ksi) double amplitude as measured by the gage at the maximum strain location (spanwise gage at trailing edge undercut). The trailing edge double amplitude tip deflection was 3.93 cm (1.55 inch). The frequency dropped from 62 Hz to 57 Hz (8%),

- Followed by 126,000 cycles at 345 MN/m^2 (50 ksi) double amplitude. Trailing edge tip deflection was 4.95 cm (1.95 inch) and frequency dropped from 57 Hz to 55 Hz at which point the test was stopped.

Evidence of a crack at the leading edge root undercut was found after the 10^6 cycle part of the test as well as a 2.54 cm (1 inch) diameter size surface delamination at the midchord convex side of the blade 8.9 cm (3.5 inch) from the bottom of the dovetail. There were also several cracks in the nickel plating on the leading edge.

6.0 WHIRLIGIG TESTING

As a means of evaluating the strength capabilities of the QCSEE composite blade under simulated engine operating conditions, several whirligig tests were conducted. These tests were conducted on four blades and are summarized as follows:

- QP004 - Whirligig Strain Distribution
- QP004 - Cyclic Testing
- QP004 - Overspeed Testing
- QP004 - 1T Fatigue Testing
- QP008 - 1F Fatigue Testing
- QP005 - Whirligig Impact
- QP011 - Whirligig Impact

Blade QP004 was utilized for four discrete tests to minimize setup and instrumentation costs.

6.1 WHIRLIGIG STRAIN DISTRIBUTION

The objective of this test was to obtain relative dynamic and steady state strain levels in several locations on the blade during rotating whirligig testing. This was accomplished using blade QP004 which was instrumented according to Figure 20. A total of 15 single-element strain gages were used for recording dynamic strains. Eight of these gages were designed to provide steady state (absolute strain level) as well as dynamic strains.

The whirligig facility used for this testing is shown in Figure 21. The instrumented blade was excited in the first three modes of vibration by ejecting air through ports in a special plate in front of the rotor. The excitation forces and resulting strain level were obtained by increasing the air pressure through the nozzles. The rotor was accelerated to the resonant frequency for each load increment and held at this point while the strain gage readouts were recorded.

During dynamic strain distribution testing the rotor was run opposite to the normal engine direction to impart maximum energy to the blade. This allowed air excitation nozzles to be directed perpendicular to the blade with the maximum relative velocity between the air and the blade. Table V lists the results of this test in the form of relative strain levels for each gage in the 1F, 2F and 1T modes. Strain gage No. 92 [at the hi-C (midchord) convex side] was the highest reading gage in first flex, gage No. 98 (leading

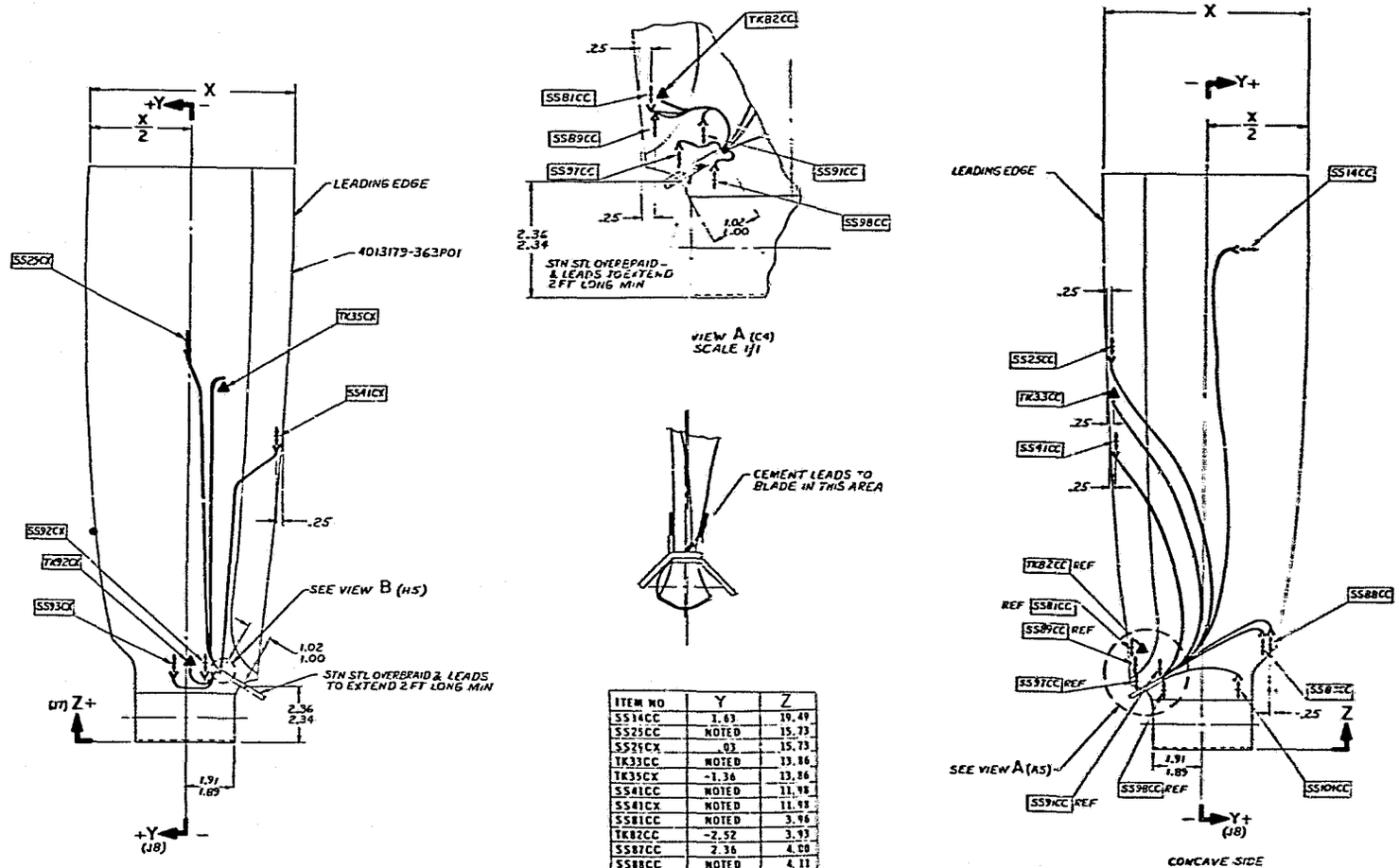

ITEM NO	Y	Z
SS14CC	1.63	19.49
SS25CC	NOTED	15.73
SS25CX	.02	15.73
TK33CC	NOTED	13.86
TK35CX	-1.36	13.86
SS41CC	NOTED	11.98
SS41CX	NOTED	11.98
SS81CC	NOTED	5.96
TKB2CC	-2.52	3.93
SS87CC	2.36	4.00
SS88CC	NOTED	4.11
SS89CC	NOTED	3.31
SS91CC	-1.71	3.35
SS92CX	-.76	3.10
TK92CX	-.135	3.10
SS93CX	.49	3.10
SS97CC	-2.21	2.58
SS98CC	-1.53	2.32
SS101CC	1.42	2.35

Figure 20. Whirligig Strain Distribution Instrumentation Location.

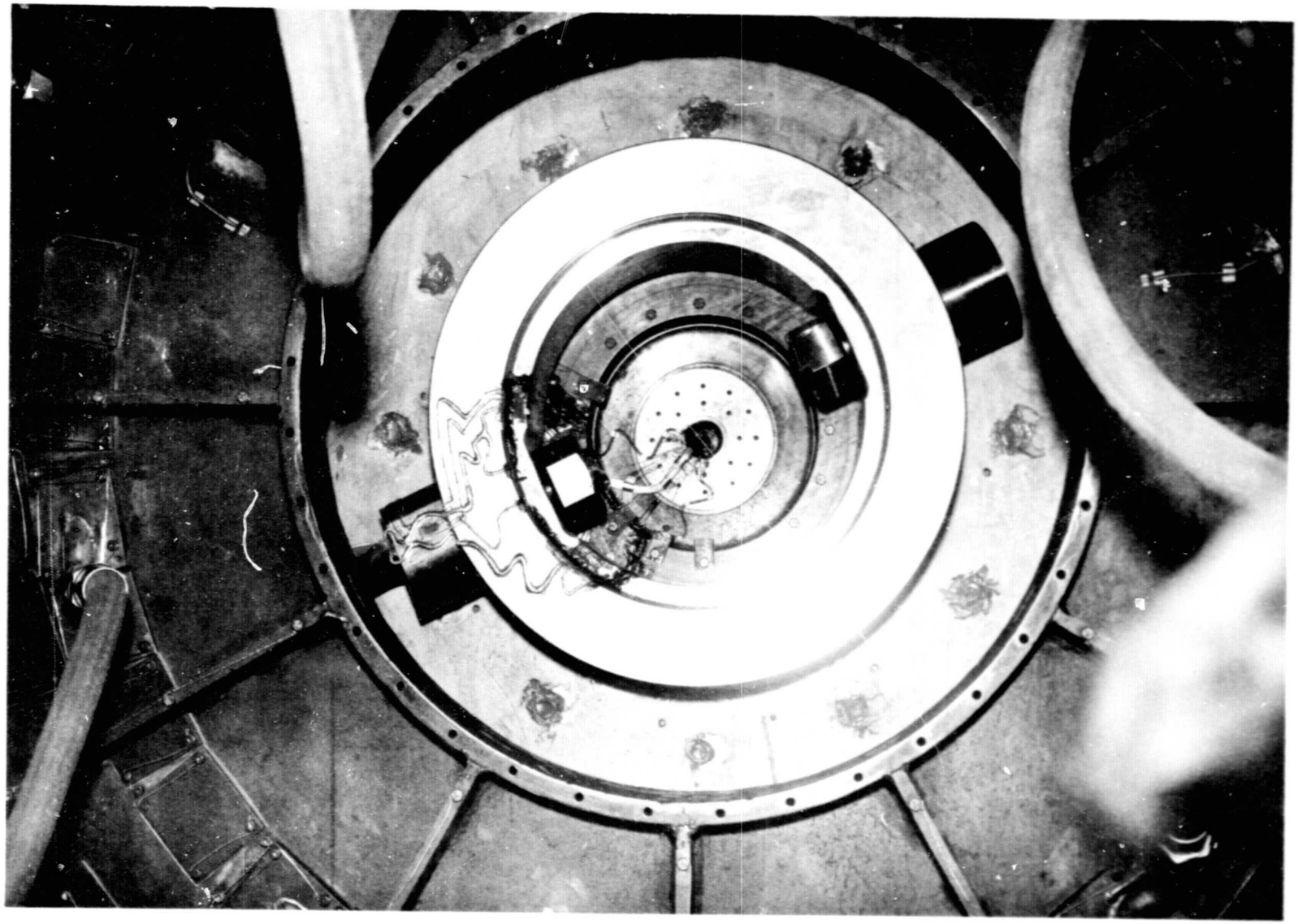

Figure 21. Whirligig Facility for Strain Distribution and Low Cycle Fatigue Tests.

Table V. Whirigig Strain Distribution; Relative Dynamic Strain Summary.

S/G	1F	2F	1T
SS14CC	9	30	15
SS25CC	8	36	56
SS29CX	29	75	55
TK41CC	13	16	23
TK41CX	10	30	65
SS81CC	53	43	31
SS87CC	35	28	36
SS88CC	60	30	10
SS91CC	57	60	48
SS92CX	100	75	44
SS93CX	56	26	20
SS97CC	17	23	19
SS98CC	73	100	81
SS101CC	68	83	100

edge root, concave side) was maximum in second flex and gage No. 101 (trailing edge root, concave side) was maximum in the first torsion mode.

Steady state centrifugal and bending stresses were also determined throughout the full speed range including overspeed. For these runs no air excitation was used. The rotor speed was increased to 100% load condition in increments of 20%. This data is summarized in Table VI. In order to compensate for strain gage output as a result of temperature effect, an apparent strain test was conducted on this blade prior to going into the whirligig. This involved heating the blade in an oven to 393° K (248° F) and recording the strain due to thermal expansion. This data was then factored into the whirligig steady state strain readings. Blade temperatures were recorded simultaneously with strain gage readings.

The test results are plotted in Figure 22, as stress versus percent load. These curves show that the peak tensile stresses in the root region are 76 to 90 MN/m^2 (11 to 13 ksi) with maximum stress appearing in the convex hi-C region. Peak compressive stresses were in the trailing edge region just above the undercut to the dovetail. These stress levels are consistent with predictions and indicate an acceptable design.

6.2 CYCLIC TESTING

After completing the dynamic and steady state stress distribution versus percent load, a cyclic test was conducted on the same blade QP004 to determine the adequacy of the blade from a low cycle fatigue standpoint. A total of 1000 simulated mission cycles was completed from an idle speed of 600 rpm to 3500 rpm (110% load). Total time to complete 1000 cycles was 37 hours. Steady state strain gages were monitored throughout the test and showed no significant variations from previous steady state runs. Posttest inspection of the blade including ultrasonic C scanning showed no damage to the blade. Blade frequencies were monitored during testing and showed no change.

6.3 OVERSPEED PROOF TESTING

After completing the cyclic proof test described in Section 6.2 an overspeed test was conducted to evaluate the capability of the blade up to 115% speed. This test was completed successfully with the blade being accelerated to 3825 rpm (115%) and held for 5-1/2 minutes. Posttest ultrasonic C Scan revealed no blade damage.

6.4 HIGH CYCLE FATIGUE TESTING

Two blades were high cycle fatigue tested in the whirligig facility to assess blade capability under vibrating loading combined with centrifugal steady state loads.

Fatigue testing was accomplished by holding the rotor speed constant at the point on a Campbell Diagram where the excitation line crosses the desired

Table VI. Steady State Stress Distribution Summary.

• MN/m^2 (ksi)

S/G No. ➡	14	25	41	87	88	91	92	93	98	101
% Load* ⬇										
20	0.7 (0.1)	12 (1.7)	-6.0 (-0.8)	-14 (-2.1)	-9 (-1.25)	11 (1.55)	20 (2.85)	9 (1.25)	17 (2.4)	13 (1.95)
40	1.4 (0.2)	18 (2.65)	-7.0 (-1.0)	-22 (3.2)	-14 (2.0)	20 (2.9)	38 (5.45)	16 (2.25)	34 (5.0)	24 (3.55)
60	1.4 (0.2)	24 (3.45)	-11 (1.6)	-30 (-4.3)	-21 (-3.0)	28 (4.05)	52 (7.5)	20 (2.85)	46 (6.7)	38 (5.5)
80	2.4 (0.35)	27 (3.45)	-8.0 (-1.1)	-36 (-5.25)	-24 (-3.5)	40 (5.8)	69 (10.0)	26 (3.8)	65 (9.4)	55 (8.0)
100	2.8 (0.4)	32 (4.65)	-7.0 (1.05)	-42 (-6.1)	-28 (-4.1)	52 (7.6)	80 (11.6)	30 (4.4)	83 (12.0)	77 (11.1)

*Average of Two Runs.

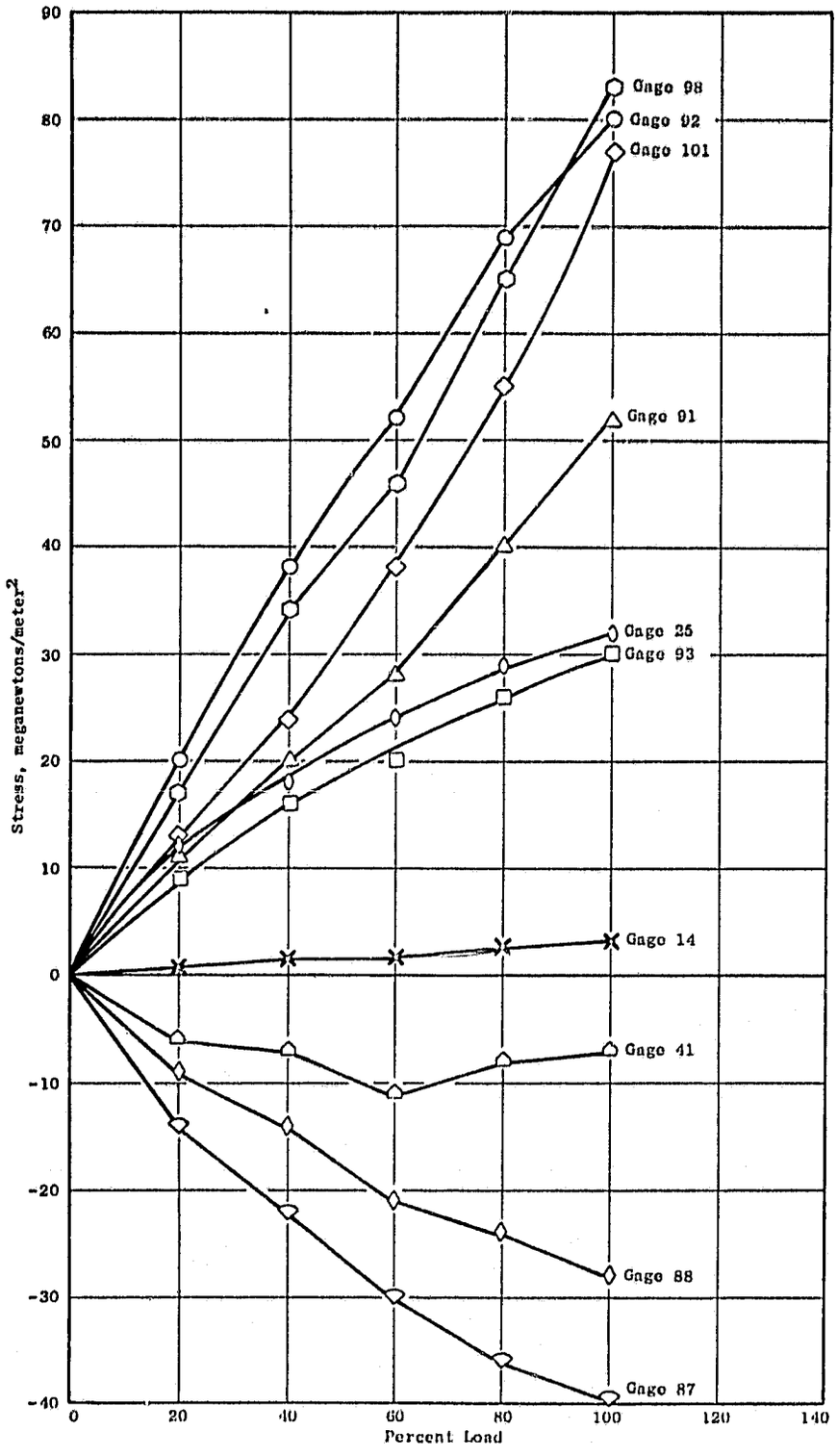

Figure 22. Steady State Stress Distribution as a Function of Load.

mode line (See Figure 23). One strain gage was at the high radial stress location as determined by TAMP analysis, and was used to establish the level of load excitation. The other gages were monitored while the blade was being excited to fatigue or until the desired number of cycles had been reached. All gages were monitored during actual cycling in the event the strain gage at the maximum strain location should fail, then a gage at a lesser strain location was used to establish the level of load excitation.

The first blade to be tested was QP004 which had previously undergone strain distribution, cyclic and overspeed proof testing. This test was conducted in the first torsion mode at a speed of 2800 rpm which corresponds to 6/rev crossover. The test was terminated after 800,000 cycles at 179 MN/m^2 (26 ksi) double amplitude maximum radial stress and 800,000 cycles at 248 MN/m^2 (36 ksi) double amplitude maximum radial stress. The frequency slowly dropped from an initial 281 Hz to 266 Hz during the 179 MN/m^2 (26 ksi) maximum stress run and further to 252 Hz during the 248 MN/m^2 (36 ksi) maximum stress run. A summary of this test along with that of blade QP008 is presented in Table VII. Damage consisted of delamination in the airfoil and root trailing edge region and some debonding of the nickel plate leading edge protection. Post test ultrasonic C-Scan results are shown in Figure 24.

Since blade failure was considered to have occurred during the first 800,000 cycles, the minimum 10^6 cycle blade strength in first torsional mode is below 179 MN/m^2 (26 ksi) double-amplitude radial stress. The type of loading, strain response and type damage indicate that the actual failure in this type of mode is a function of shear stresses within the blade. However, the surface stress measurements can be used as a guide to determine the level of allowable shear stresses since the shear stress will be proportional to the radial surface stress. The TAMP analysis shows that a shear stress of 43 MN/m^2 (6.3 ksi) occurs near the hi-C location at the maximum surface radial stress of 179 MN/m^2 (26 ksi). Fatigue failure after 800,000 cycles at this level appears reasonable.

The second high cycle fatigue test was conducted in the first flexural mode on blade QP008. This blade was excited at a 2/rev crossover speed of 2400 rpm. The initial peak double amplitude stress was taken at 186 MN/m^2 (27 ksi) at the maximum stress location. The blade successfully completed one million cycles with no loss in frequency. Double amplitude stress was increased to 248 MN/m^2 (36 ksi) where the blade frequency dropped from 79 Hz to 75 Hz after one million additional cycles. The blade frequency further dropped to 71 Hz after 90,000 cycles at 345 MN/m^2 (50 ksi) and the test was terminated. This data is also reported in Table VII. Posttest C-Scan results are given in Figure 25.

The results of this test and the bench high cycle fatigue tests were used to establish the stress range diagram for the final blade analyses. The analysis shows satisfactory margin for safe engine operation.

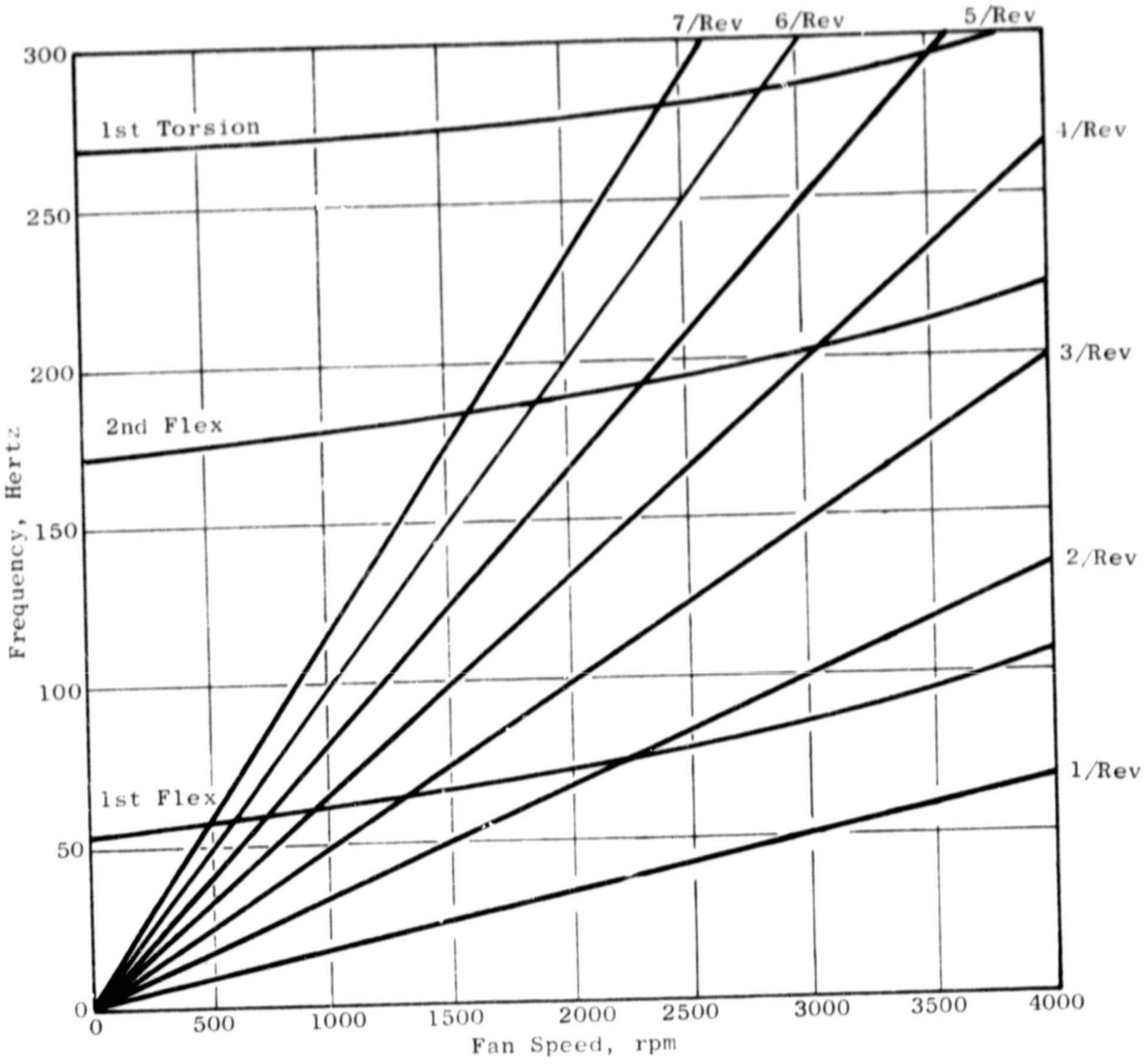

Figure 23. Campbell Diagram; UTW Preliminary Design, Composite Blade.

Table VII. Whirigig High Cycle Fatigue Test Summary.

S/N	Mode	Speed rpm	Hertz Frequency		Max. Strain Gage	Double Amplitude Stress MN/m^2 (ksi)	No. of Cycles x 10^6
			Start	End			
QP004	1T	2800	281	266	101	179 (26)	0.8
	1T	2800	266	252	101	248 (36)	0.8
QP008	1F	2380	79	79	92	186 (27)	1.0
	1F	2380	79	75	92	248 (36)	1.0
	1F	2380	75	71	92	345 (50)	0.09

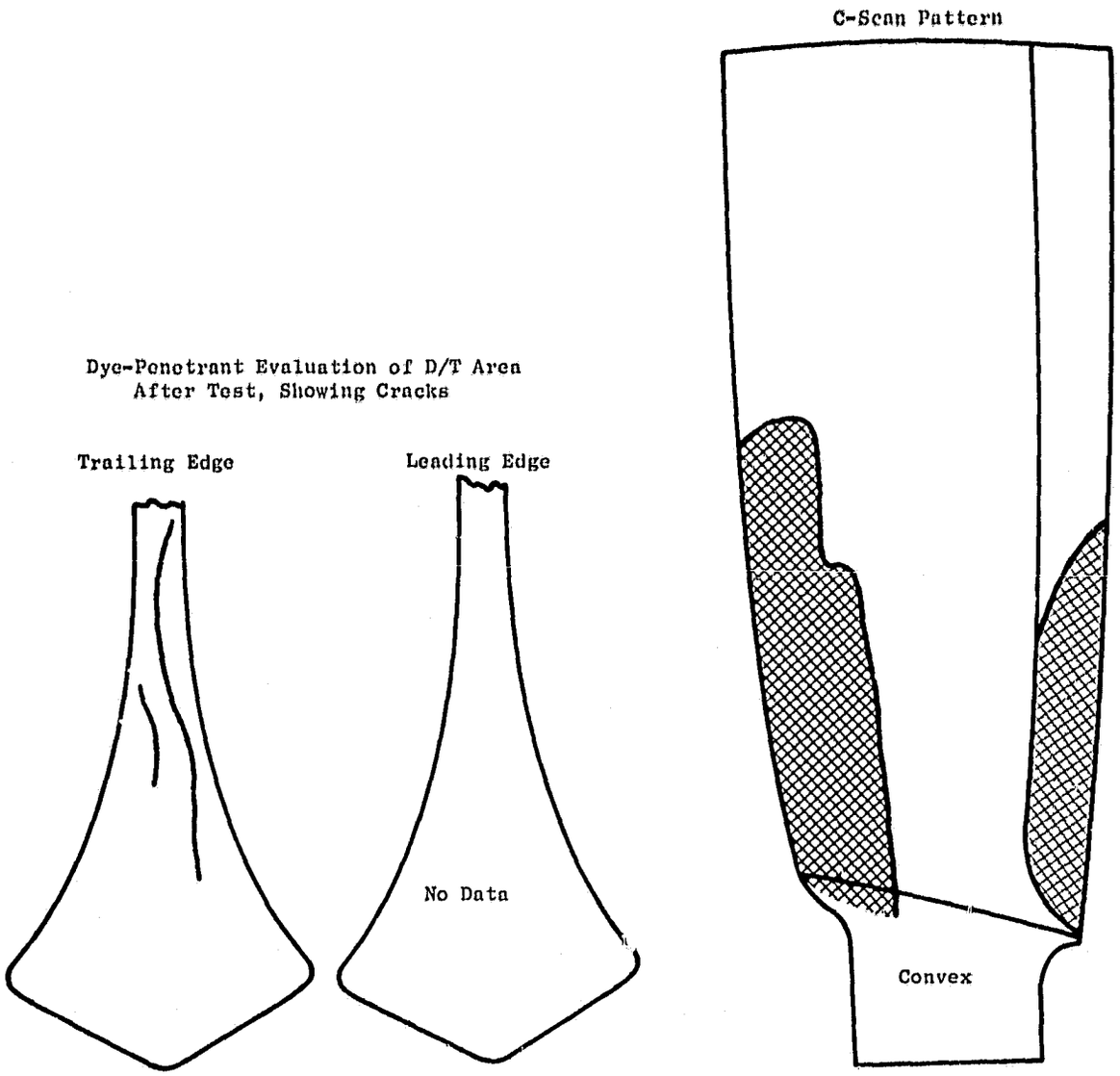

Figure 24. High Cycle Fatigue Posttest Evaluation; Blade S/N QP004.

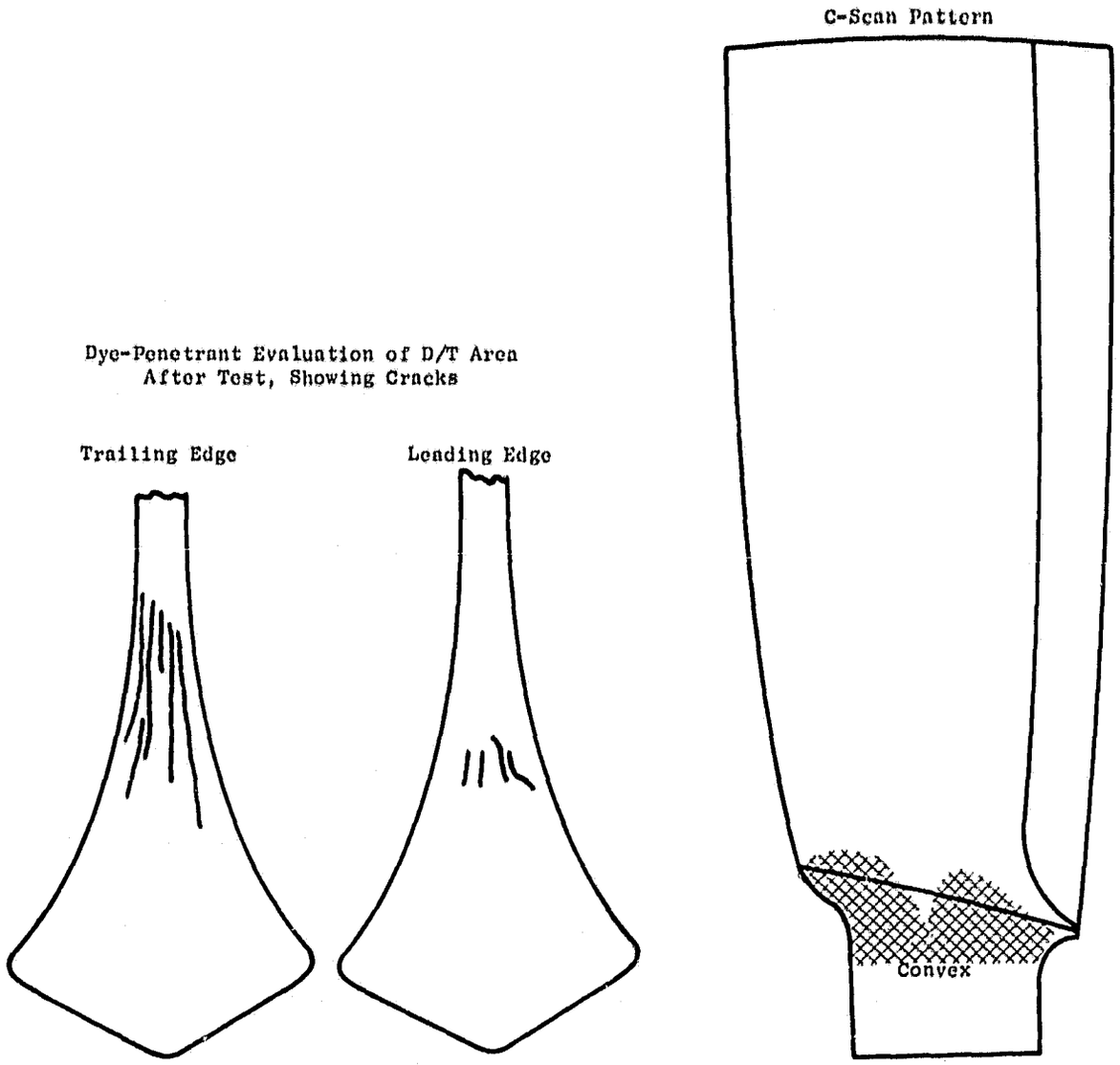

Figure 25. High Cycle Fatigue Posttest Evaluation; Blade S/N QP008.

6.5 WHIRLIGIG IMPACT

In order to determine the impact capability of the UTW composite fan blades from the ingestion of 0.9 Kg (2 lb) birds, two whirligig impact tests were conducted. Blades S/N QP005 and QP011 were impact tested, one at a time in the whirligig facility shown in Figure 26.

The facility consists of a 700.5 kW (1000 horsepower) drive motor, a variable speed output magnetic clutch, a speed increasing gearbox, and a horizontal drive spindle shaft to the rotor.

The rotor was soft mounted for these tests to lessen possible rig damage should blade failure occur following impact. The disc was provided with two opposing spindles, one for the composite blade and the other for counterbalance weight. The blade spindle was positioned for proper incidence angle for impact. This is shown in Figure 27.

The environmental chamber was made with three camera ports, located at the top, side and directly in front of the rotor, to permit high speed motion pictures to be taken from several angles simultaneously.

The lighting was provided by thirty-two 1000 watt (GE Par 64) spotlights mounted on the outside of the environmental chamber and directed through individual glass ports. The blades and background were appropriately painted to reflect the light and provide contrast.

The blades were impacted with a simulated (RTV) bird injected automatically into the path of the blade at a rotor speed of approximately 3255 rpm [303 m/sec (1010 ft/sec) tip speed]. The "Fixed Bird" technique was used to set the impact bite. This means that the bird was securely fixed to a mechanical injecting system which could insert it at a set depth into the path of the rotating blade and retract it subsequent to impact. Basically the mechanism consisted of a cup (bird carrier) attached to the end of a spring loaded shaft which was supported and free to slide in the ball bushings. It was actuated by firing an explosive bolt which held the shaft (and spring) in the retracted (cocked) position. The particular springs that were used provided a maximum stroke of 7.6 cm (3.0 in.) in 10 milliseconds. This yielded a maximum bite size of 6.35 cm (2.5 inches) allowing 1.25 cm (0.5 inches) clearance between blade and bird.

In order to obtain the required bite, the explosive bolt had to be fired when the rotor was at the required speed, but at an instant which would permit the blade to reach the impact point at the same time the bird reached the desired depth (full stroke). In addition, the camera and lights had to be activated to catch the event.

Figure 28 shows the block diagram of the firing system used to trigger the events and fire the bolt at the proper time. The operating sequence for the system is outlined on the following page.

Figure 26. Whirigig Impact Facility.

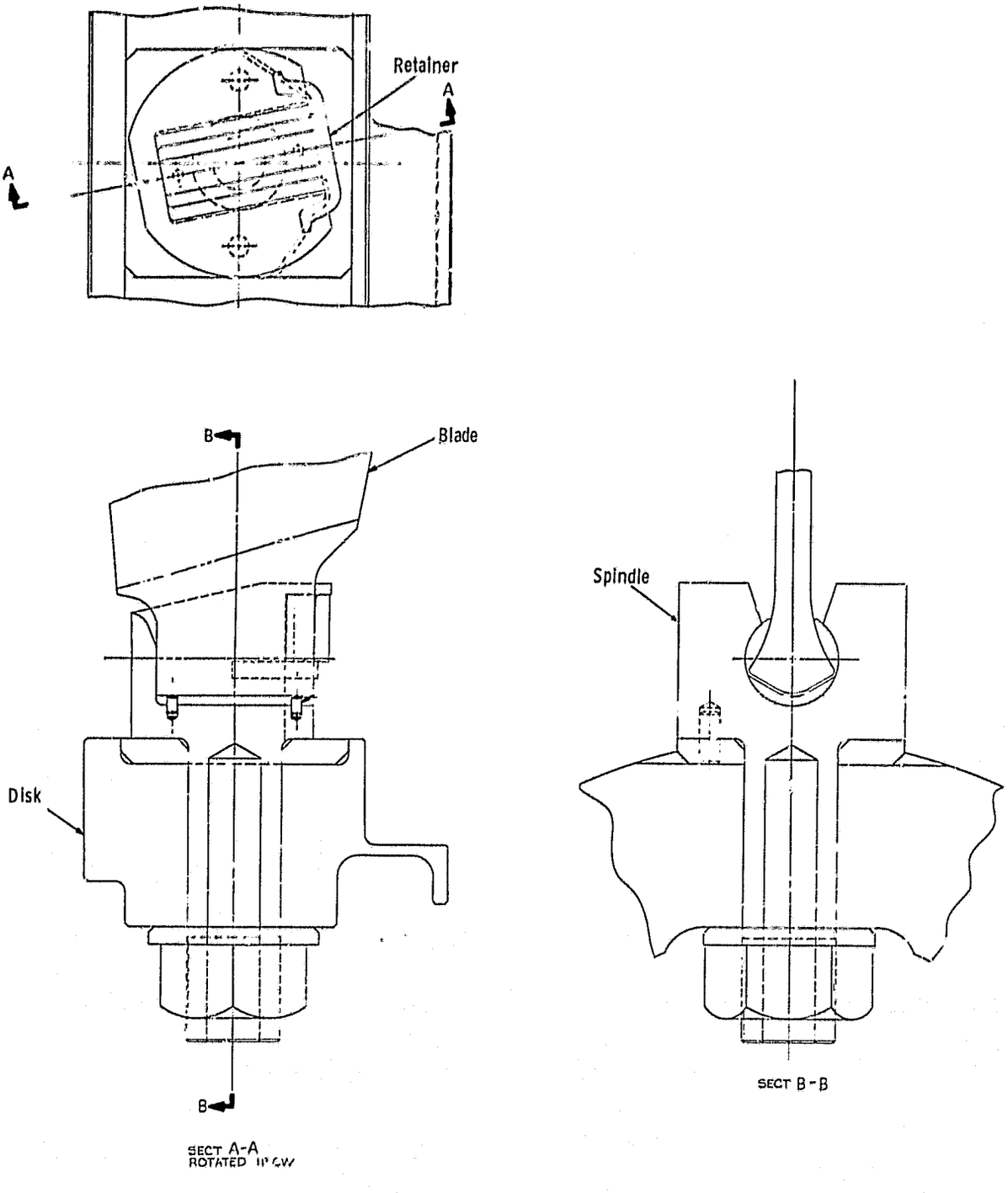

Figure 27. Whirigig Rotor Assembly, QCSEE Impact Tests.

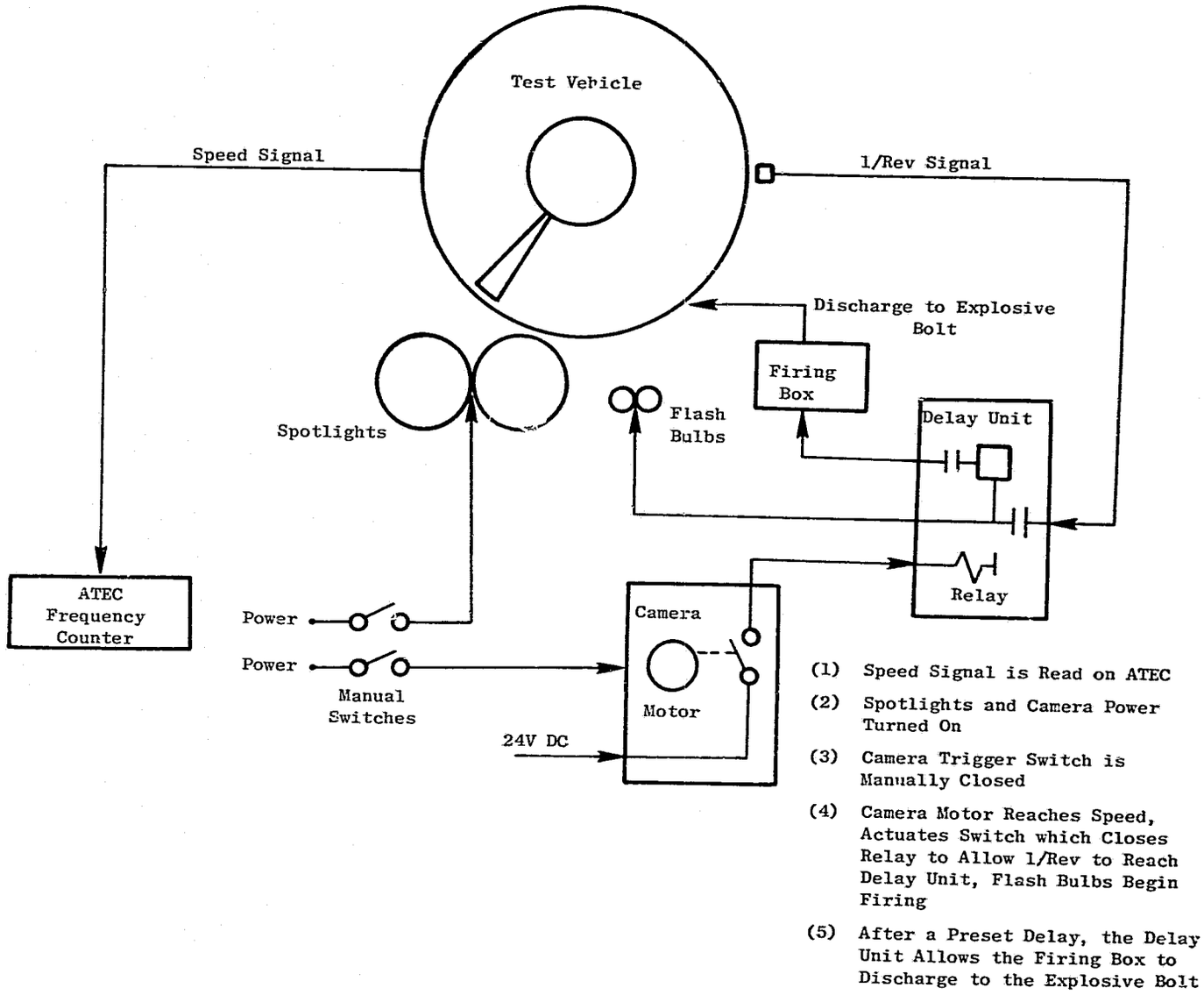

Figure 28. Firing Sequence; Whirigig Impact Tests.

1. The rotor speed signal was fed to a frequency (ATEC) counter. When a speed of 3255 rpm was set, the cell operator turned on the spotlights and closed the trigger switch, starting the cameras.

2. When the control camera reached operating speed, it tripped a microswitch which completed a circuit to essentially permit the 1/rev signal to reach the delay unit. This signal also began firing four sets of sequenced flash bulbs.

3. After a preset delay has occurred, allowing the flashbulbs to reach maximum lighting intensity, the delay unit discharges, causing the bolt to explode.

The injector was positioned for the proper depth slice at the correct span for each blade tested. For all impacts the mechanism was adjusted such that the centerline of the bird was 9.65 cm (3.8 inches) from the blade tip (80% span).

With the bird attached and the mechanism cocked, the drive was accelerated to approximately 1200 rpm, at which point the camera power was turned on. The acceleration was then continued until 3255 rpm was reached. At this point, the cell operator turned on the spotlights, armed the explosive bolt, and started the firing sequence. The rotor was decelerated immediately after impact to minimize possible secondary damage and damage to the vehicle. The blade was then removed and still photographs taken. Blade photographs are shown in Figures 29 and 30. The RTV simulated bird used in this test is shown in Figure 31.

A summary of the test results for both tests is presented in Table VIII. The conditions chosen for this test represent the ingestion of a .908 g/kg (2 pound) bird at aircraft takeoff conditions. The objective slice size of .369 kg (13 ounces) was not achieved on the first test.

Posttest evaluation of both blades was performed after impact testing. Blade QP005 was sectioned to aid evaluation. The outer 1/3-span of the blade delaminated generally along the interface of plies. The lower 2/3-span separated into three pieces, an inner core of Kevlar-49 laminate and two outer shells of Boron/Kevlar-49 interply laminate. The three pieces show little distress except at the top of the outsert where considerable delamination occurs. The delamination stops abruptly in the outsert.

The test results of QP011 indicated a deficiency in local impact capability which resulted in a considerable blade weight loss. After the completion of these tests reassessment of the whirligig impact test program was made and it was decided to eliminate the additional planned impact testing until improvements in local impact capability had been completed. These improvements would be identified through other ongoing programs with the possibility of incorporation into QCSEE at a later date.

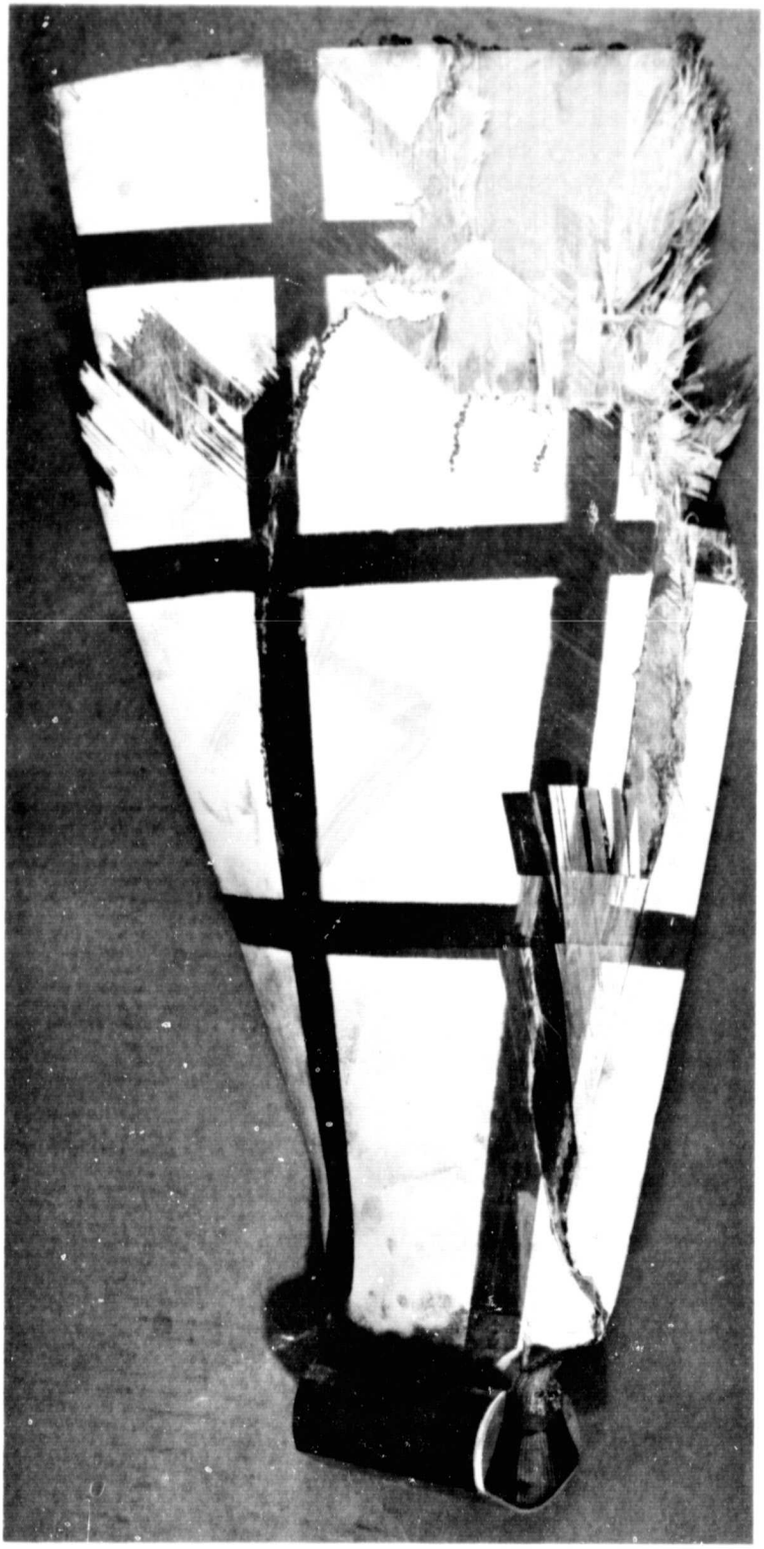

Figure 29. Convex Side of Impact Test Blade QP005 Following Test.

Figure 30. Simulated (RTV) Bird used for Whirigig Impact Test Showing Slice.

Figure 31. Concave Side of Impact Test Blade QP005 Following Test.

Table VIII. Whirigig Test Results Summary.

Incidence Angle 33°, 75% Span, 1010 ft/sec

S/N	Resin	Material	Layup	Slice g (Oz.)	% Wt. Loss
QP005	PR288	Kevlar-49/Boron	0/+45/0/-45	227 (8)	7
QP011	PR288	AU/Boron/Kevlar-49	0/+45/0/-45	369 (13)	77

7.0 CONCLUSIONS

The completion of the QCSEE preliminary composite blade test program provided the following conclusions:

- Blade frequencies and mode shapes are close to predictions and are within the design tolerance.
- The preliminary blade design satisfies all strength requirements of the program with the exception of impact strength capability which is being improved on other NASA and related programs.